# Final Project Report

On

# Oil Recovery with Novel Skimmer Surfaces under Cold Climate Conditions

to

Coastal Response Research Center,
Cooperative Institute for Coastal and Estuarine Environmental Technology,
Prince William Sound Oil Spill Recovery Institute

and

Department of the Interior, Minerals Management Service

Arturo A. Keller and Kristin Clark
3420 Bren Hall
Bren School of Environmental Science & Management
University of California
Santa Barbara. CA, 93106-5131
Phone: 805-453-1822
Email: keller@bren.ucsb.edu

**Abstract**

Increasing oil exploration, production and transport in Arctic waters will increase the risk of an oil spill occurring in cold and ice-infested waters. The mechanical oil spill recovery equipment currently used in warmer waters was not designed to collect much more viscous oils, or oil-ice mixtures. The presence of ice crystals in oil emulsions affects the adhesion processes between an oil slick and the surface of an oleophilic skimmer and prevents oil from being efficiently recovered. Novel drum skimmer surface geometry and materials, tailored to the conditions present under cold climates, are expected to significantly increase the rate of oil recovery, reducing cost and risk.

The objective of this project was to perform a comprehensive analysis of the adhesion between oil or ice-in-oil mixtures and various surface patterns and materials, under cold climate conditions. This knowledge was then applied to improve existing mechanical response equipment so that it can be applied efficiently under these conditions. The novel recovery surfaces that proved to increase the recovery efficiency of a drum skimmer up to two times in warm waters were also successful in cold climate conditions.

In the first phase of the project, laboratory bench-scale tests of different surface materials were conducted, to determine contact angle and amount of oil adhered at sub-freezing conditions, with and without ice. It became clear that the physicochemical property that would be most significantly influence by cold climate conditions would be viscosity, and that the presence of ice would also have an important effect on viscosity, although to a varying degree depending on the initial oil viscosity. Neoprene was the best material surface, of those tested here, for adhering oil even under oil/ice conditions.

Based on the results of the laboratory tests at subfreezing conditions, we selected materials and surface patterns with the highest oil recovery potential under cold climate conditions, and performed field scale oil spill recovery tests with three different oils at the U.S. Army Corps of Engineers Cold Regions Research and Engineering Laboratory (CRREL), located in Hanover, NH. This provided valuable information about the correlation between the laboratory tests and full scale experiments. It also demonstrated the potential of the skimmer modifications under conditions similar to response operations. The field tests were very successful, with high rates of oil recovery under cold climates, with and without ice present. However, the presence of ice does decrease the overall rate of oil recovery to some extent.

These studies served to advance the goals of the Coastal Response Research Center, the Prince William Sound Oil Spill Recovery Institute, and the Minerals Management Service by providing important information for the improvement of cleanup of oil spills in cold climates. The outcome of this project advanced our understanding of the adhesion of oil and oil emulsions (water containing and ice-containing) to recovery surface material under cold climate conditions. This research will facilitate selection of materials and surface configurations that result in significantly higher recovery rates of oil spills in cold and ice-infested waters. This will ultimately lead to a faster oil spill cleanup and greater protection of natural resources.

## 1. Problem Statement

According to the U.S. Environmental Protection Agency (USEPA), almost 14,000 oil spills are reported each year in the United States alone. The considerable increase of oil exploration and transport in Arctic waters will increase the risk of an oil spill occurring in cold and ice-infested waters. Currently, mechanical oil spill recovery in cold climates is inefficient largely due to the fact that the equipment available to oil spill responders was not designed to collect very viscous oils and oil-ice mixtures. The presence of ice crystals in oil emulsions affects the adhesion processes between an oil slick and the surface of an oleophilic skimmer and prevents oil from being efficiently recovered. Oil spill responders have used weir type skimmers and large vacuum hoses to suck in oil-ice mixture, resulting in a significant amount of free water in the recovered product, reducing oil spill recovery efficiency and creating a discharge problem.

Oleophilic skimmers are based on the adhesion of oil to the rotating skimmer surface. The rotating surface lifts the oil out of the water to an oil removal device (e.g. cleaning blade, roller, etc.). The materials used to manufacture the surface of adhesion skimmers have not been adapted to the special conditions in cold climates. Steel, aluminum, and general-use plastics had been in use for more than 25 years. Material selection has not been based on the adhesive properties, but rather on historical practice, price and availability. Very little effort has been made to study the affinity of new materials for oil and the recovery efficiency under cold climate conditions. Research conducted in our laboratory indicates that the recovery material on the skimmer surface can change the recovery efficiency up to 20%, and that tailoring the geometry of the skimmer surface can have much higher recovery efficiencies, even up to 200%. To date we have only studied oils and water-in-oil-emulsions at temperatures above 0°C. All the oils tested were above their Pour Point. No ice-in-oil emulsions were tested. To our knowledge, no scientific research has been done to study the effect of changes in oil properties at cold temperatures and/or in the presence of ice in oil emulsion on oil adhesion to the material of the recovery surface. Our research aims at studying this process in detail.

Various shapes of the recovery unit, such as a mop, belt, brush, disc, and drum, have been developed to increase skimmer efficiency. Our research has shown that the relatively low recovery rate of smooth drum, belt and disk skimmers can be explained by their relatively small surface area. Only a limited amount of oil adheres to the recovery surface in every rotation, requiring more time or more skimmers to increase the overall recovery. Brush and mop skimmers attempted to address this issue by increasing the surface area in contact with oil. Although these skimmers allow more oil to adhere to the recovery surface, not all the adhered oil can be removed from the bristles. Thus, a significant fraction of the oil remains on the bristles, reducing the overall recovery efficiency.

The oil spill recovery process is composed of two equally important goals. The first one is to remove oil from the water surface and the second one is to remove oil adhered to the recovery surface and transfer it into to a collector. The recovery efficiency depends on the achievement of both of these goals. In case of a smooth surface (e.g. smooth drum, disk or belt), the amount of oil recovered from the water surface is relatively low, but close to 100% of it can be removed by a cleaning blade. In the case of a brush surface, the recovery of oil from the water surface is high on the first pass, but a significant amount of oil remains on the surface, reducing the overall recovery rate.

The characteristics of an adhesion skimmer surface pattern and materials that can significantly increase oil recovery efficiency can be summarized as follows:

It should have the maximum surface area possible for a given width of the recovery surface;

- The formation of oil menisci is highly desirable, since this allows a thicker layer of oil to be recovered from the water, and it slows oil drainage back into the oil spill;
- The cleaning blade should be able to remove close to 100% of the oil adhered to the recovery surface;
- The surface pattern and materials should be tailorable to the oil properties of a particular region (e.g. Alaskan crudes);
- The recovery surface pattern and materials should take into consideration the changes in oil properties that occur as the oil weathers, and in colder climates.

With these goals in mind, a surface pattern that satisfies all these criteria has been developed in our laboratory. The materials used as the contact surface have been selected based on their ability to adhere to oil, their durability and relatively low swelling, and feasibility of implementation in existing skimmers. The basic configuration of the recovery surface is shown in Figure 1.

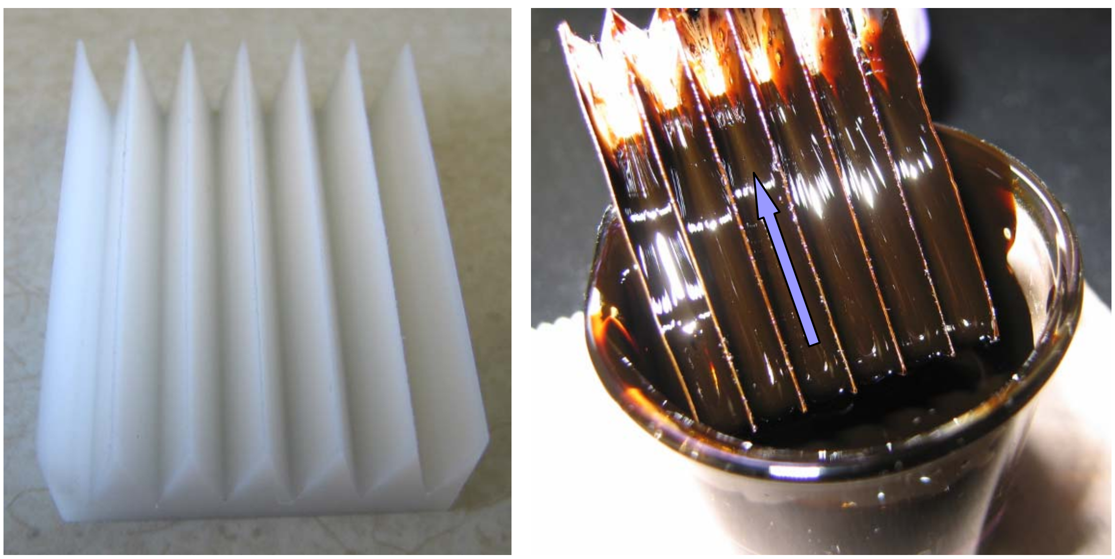

**Figure 1. V-patterned recovery surface. The arrow indicates the direction of oil recovery.**

A V-patterned surface maximizes the surface area of a drum, belt or disc skimmer (Broje and Keller, 2006). Depending on the angle and the depth of the channels, the surface area can be increased 2-4-fold for the same width of recovery surface. It also allows menisci to be formed in the depth of the channel, increasing the amount of recovered oil and slowing down oil drainage. The variation in channel width with depth allows efficient use of this surface pattern on oils with a wide range of viscosities. The lighter oils will be collected in the depth of the channels, while viscous oils can be collected in a wider part of the channel allowing water drainage in the deeper part of the groove. The cleaning blade can be machined to almost perfectly match the recovery surface. Thus, close to 100% of the recovered oil can be removed and transferred into the oil collector in every rotation. Figure 2 shows two grooved drums installed into a standard drum skimmer (Elastec/American Marine Mini Max®)

**Figure 2. Mini Max® drum skimmer. Standard drums were replaced with grooved drums and a matching cleaning blade.**

Recent tests conducted at Ohmsett – The National Oil Spill Response Test Facility, located in Leonardo, NJ, have shown that V-patterned drums yield to 2 to 3 times higher recovery efficiency compare to the conventional smooth drums (Broje and Keller, 2007a). This is illustrated in Figure 3. Different materials on the drum surface may have higher oil recoveries (Broje and Keller, 2007b).

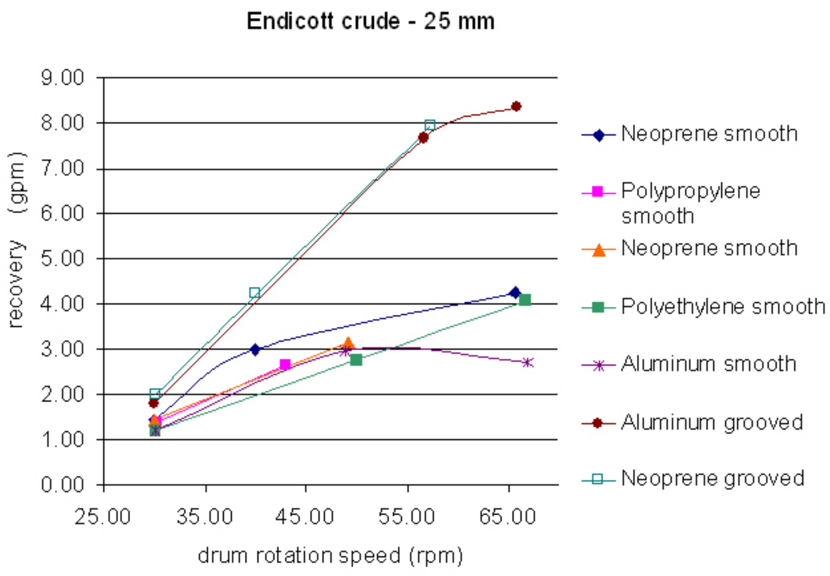


**Figure 3. Comparison of recovery rate between flat (smooth) and grooved drums.**

## 2. Objectives

The data presented in Figure 3 indicate that the use of grooved drums instead of conventional drums can more than double the oil spill recovery efficiency in warm waters (10-30 $^oC$). This includes the recovery of very light hydrocarbon mixtures such as diesel. We believed that this surface pattern could be successfully used in the cold climate conditions. There were several aspects that need to be studied in this respect, including the effect of:

- Cold temperatures on the recovery of viscous oils by smooth and grooved drums;
- Slush ice mixed with oil on the adhesion process between oil/ice and the surface of the recovery unit;
- Material and geometry of the recovery unit on oil withdrawal and slip condition;
- Drum rotation speed on the adhesion process, amount of recovered oil and recovered free water.

The objective of this project was to perform a comprehensive analysis of the adhesion processes between oil or ice-in-oil mixtures and various surface patterns and materials that are being used or proposed for use in oil skimmers, under cold climate conditions. This knowledge can be used to develop mechanical response equipment that can be efficiently used under these conditions.

We studied the properties of oils (in particular, viscosity, pour point and density) with increasing ice content. We evaluated how the formation of oil-and-brash-ice mixtures, with various amounts of ice, affected the adhesion and recovery efficiency of the mixture. We tested various materials (polymers and metals) and surface configurations (smooth and patterned surfaces) in order to identify materials and configurations with the highest recovery efficiency under variable conditions. The surface pattern presented in Figure 1 was modified to examine the effect of channel angle and depth, surface material, and roughness on the recovery efficiency of various oils. Crude oil and oil-ice mixtures, as well as refined products such as diesel and HydroCal, were used for these studies.

Following the laboratory tests, we selected the materials and surface patterns that performed best under cold climate conditions, and performed full scale oil spill recovery tests at CRREL. This will provide us with valuable information about the correlation between the laboratory tests and full scale experiments, as well as demonstrate the potential of the proposed skimmer modifications under conditions similar to response operations.

## 3. Methods

### 3.1 Laboratory work

#### 3.1.1 Physicochemical Properties of oils

The four most relevant physicochemical properties for understanding oil recovery from surface water spills are density, viscosity, surface tension and dynamic advancing contact angle.

##### 3.1.1.1 Density

A Pyrex specific gravity bottle for viscous fluids was used to determine the density of the oil according to ASTM D70 and D1429. The mass of the oil or oil and ice mixture was divided by the volume of the specific gravity bottle to determine the density. All weights were measured on a Mettler Toledo analytical balance to four decimal places. The volume of the specific gravity bottle was calibrated with water at a known temperature and density, which ranged from 29 to 33 mL depending on the temperature at which the samples were measured.

##### 3.1.1.2 Viscosity

A Brookfield DV-II+ Pro Programmable Viscometer (Figure 4) was used to analyze the viscosities and percent torques of the oil samples. For each run approximately 250 mL of sample were analyzed in a container 120 mm high and with a minimum diameter of 82.6 mm. The speed and spindle used were also recorded for consistent measurements of samples. Diesel required a small sample adapter due to the low viscosity of the non-Newtonian liquid. An average viscosity was measured from five separate locations in the container.


**Figure 4. Brookfield Viscometer.**

#### 3.1.1.3 Surface tension

A Thermo Cahn Radian 315 (Figure 5) was used to measure the surface tension according to the manual. This measurement was made with a Du Nouy ring (Figure 6) and repeated five times to obtain an average value. The ring was cleaned in between runs with solvent (hexane, methylene chloride, toluene, or ethanol) or a deionized (DI) water rinse, depending on the oil. Excess solvent was burned off. A calibration factor was used to correct for imperfections in the ring. This was derived from the known surface tension of water and the measured value of surface tension with the ring; at 25 $^{o}$C the surface tension of water is 72.0 mN/m. The correction factor was 1.04 for the ring used in these experiments.


**Figure 5. Thermo Cahn Radian 315.**

**Figure 6. Du Nouy ring.**

### 3.1.1.4 Dynamic advancing contact angle

To analyze the affinity of test oils to various recovery materials and to identify the material with the highest recovery potential, we used a Dynamic Contac Angle analyzer (Thermo Cahn Radian 315), available in our lab through funding provided by the Minerals Management Service (MMS). Contact angles of liquids on solid surfaces are widely used to predict wetting and adhesion properties of these solids by calculating their solid-vapor surface tension. This method was widely discussed in the literature (e.g. Wake, 1982). The Dynamic Contact Angle (DCA) analyzer overcomes the limitations of static contact angle measurement devices by measuring much larger surfaces on liquid solutions rather than single drops on a plate. This eliminates the risk of concentrated contaminants or incomplete profiles. The DCA analyzer operates by holding a plate in a fixed vertical position, attaching it to a microbalance and moving a probe liquid contained in a beaker at constant rate up and down past the plate. A unique contact angle hysteresis curve is produced by the microbalance as it measures the force exerted by the moving contact angle in advancing and receding directions (Figure 7). The dynamic contact angle is then calculated from the modified Young's equation (Wilhelmy equation)

$$\Theta = \cos^{-1} (F/\gamma p) \qquad (1)$$

where $\Theta$ is the contact angle, F is the applied force, $\gamma$ = surface tension, and p is the wetted perimeter.

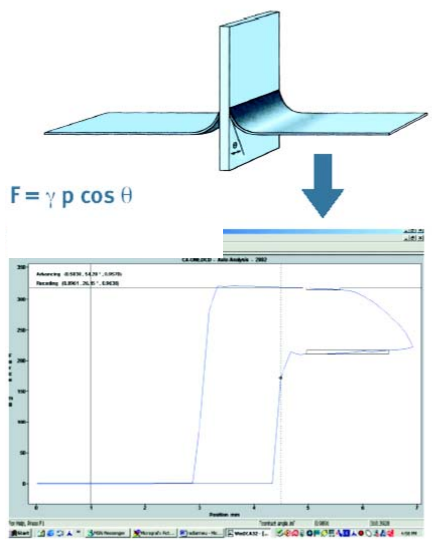


**Figure 7. Dynamic contact angle analysis (Thermo Electron Corporation)**

The advancing contact angle measures the affinity between the liquid and solid surfaces. A smaller contact angle indicates that the liquid will wet the surface more easily. A 0° angle represents complete wetting while a 180° angle represents complete non-wetting. The difference between the advancing and receding contact angles is called the contact angle hysteresis. This parameter measures the ability of the solid surface to retain molecules of liquid during the receding phase. If liquid remains on the surface after the surface is withdrawn from the oil, the receding contact angle is 0°. Oil recovery is measured as the weight of adhered oil per unit surface area.

The Dynamic Contact Angle analyzer has been successfully used by other researchers to study wetting and adhesion properties of various surfaces (e.g. Lee et al., 1998 and Della Bona, 2004). The DCA will allow us to select the surface pattern and materials that have the highest oil spill recovery potential based on the advancing contact angle and contact angle hysteresis.

The Thermo Cahn Radian 315 was used to determine the contact angle between the materials and the oils. A minimum of five measurements were run and averaged. The receding speed was 20μm/s and the advancing speed was 80μm/s. Each piece of material was cleaned and dried according to previous studies (pre-wash with soap and water, rinse with water, wash with ethanol, rinse with DI water and blow dry with nitrogen gas). The uncompressed width and thickness were recorded and inputted into the system configuration settings.

### 3.1.2 Oil recovery of various materials

The Thermo Cahn Radian 315 (Figure 8) was also used to determine the recovery of oils with different materials. A minimum of five measurements were run and averaged. The receding speed was 20μm/s and the advancing speed was 80μm/s. Each piece of material was cleaned and dried according to previous studies (pre-wash with soap and water, rinse with water, wash with ethanol, rinse with DI water and blow dry with nitrogen gas). The uncompressed width and thickness were recorded. Small squares 25 x 25 mm were cut from each material. After attaching them to the DCA’s clamp, the automated procedure for dipping the sample into the oil was performed. The sample was dipped precisely 20 mm into the oil. The software (WinDCA) provided with the Thermo Cahn Radian 315 recorded the start and finish position of the material. Based on the mass at the final position of the run relative to the mass at the start position, the recovered mass of oil can be determined. Oil recovery was normalized by the area of the material that was in contact with the oil, which was determined by using the perimeter of the area times the depth the material is submerged, approximately 2 x (1.59 mm + 25.00 mm) x 20 mm. The same procedure was used for oil/ice mixtures.

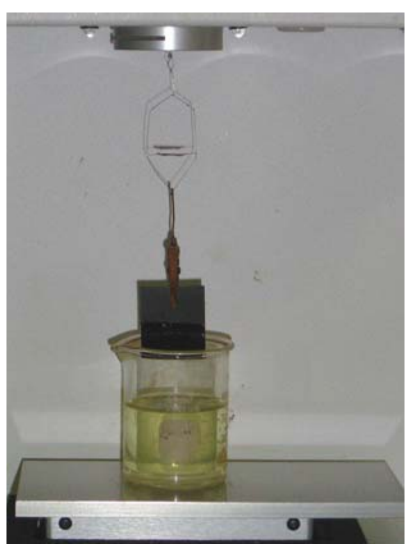

**Figure 8. Thermo Cahn Radian 315 measuring oil recovery.**

### 3.1.3 Oil-ice mixture preparation

Filtered sea water from the Santa Barbara Channel with a salinity of about 33.6 ppt was collected. The sweater (2.00 L) was poured into a plastic pan to achieve a thickness of 38.1 mm. The pan was covered with foil and left overnight in a -20ºC freezer. Four inch by two inch chunks were loaded into the chute flush of a mechanical ice shaver (Figure 9), against the blade, to achieve uniform shaved ice particles (Figure 10).

**Figure 9. Mechanical ice shaver**

**Figure 10. Shaved ice**

## 3.2 Full scale test at the Cold Regions Research and Engineering Laboratory (CRREL)

### 3.2.1. Test Set-up

Testing was conducted in the Material Evaluation Facility (MEF) at CRREL (Figure 11). The MEF is 14 by 6.7 m with 4 m ceiling that can be maintained as low as –50 ºC ±1 ºC. A test tank was built inside the MEF specific for these tests. The test tank was approximately 3 by 3m tank filled with around 5,000 L of seawater created using sea salt, with a total salinity of 35 ppt. The bottom and side of the tank was insulted with 50 mm thick Styrofoam insulation to minimize unintended ice formation. Two pipe connections on the bottom of the tank were also available for supplemental water heating to maintain water temperature. Ice chips generated using a grinder were distributed during specific tests on the oil surface to evaluate the efficiency of the skimmer in a frazil ice environment.

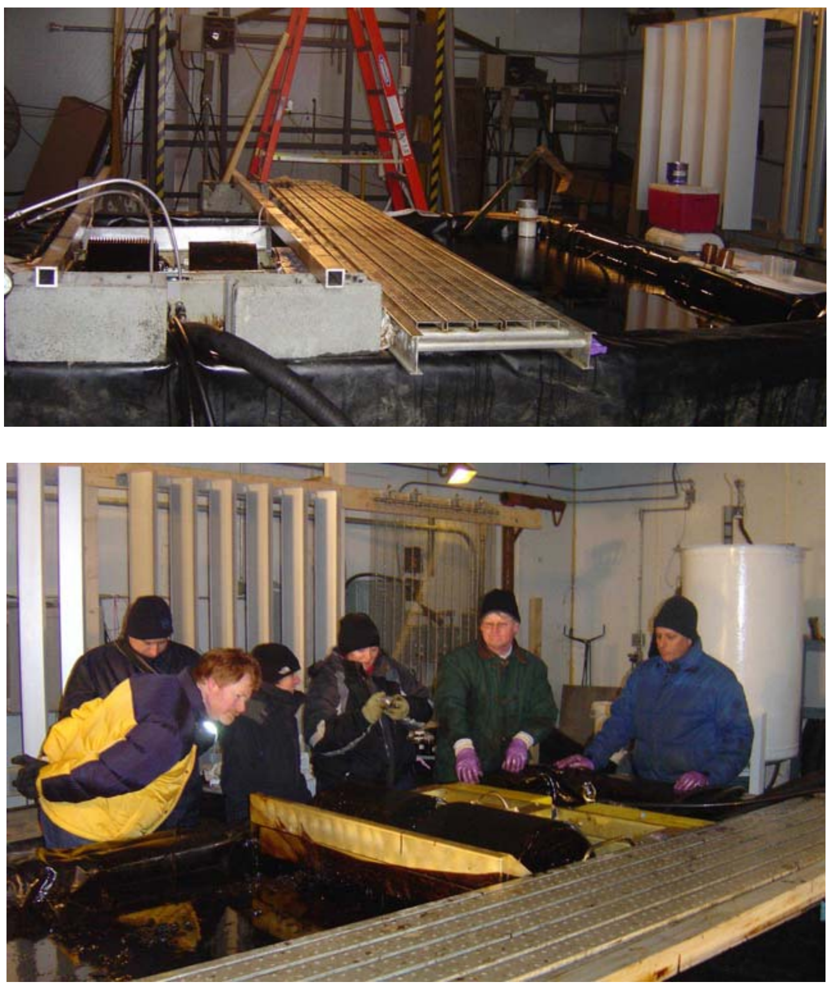

**Figure 11. MEF facility at CRREL (a) test tank with Mini Max skimmer; (b) skimmer operation during recovery tests.**

The test tank was deep enough to allow for the operation of the drum skimmer systems, but small enough to provide good access to and observation of the test set-up. A similar setup was used at Ohmsett for field scale tests in August and October 2005 (Figure 12). An Elastec Mini-Max® drum skimmer was used, so that the results could be compared to the higher temperature tests. Since the recovery efficiency depends mostly on the design of the drum surface and cleaning blade, the results from these tests are easily transferable to other commercial skimmers.

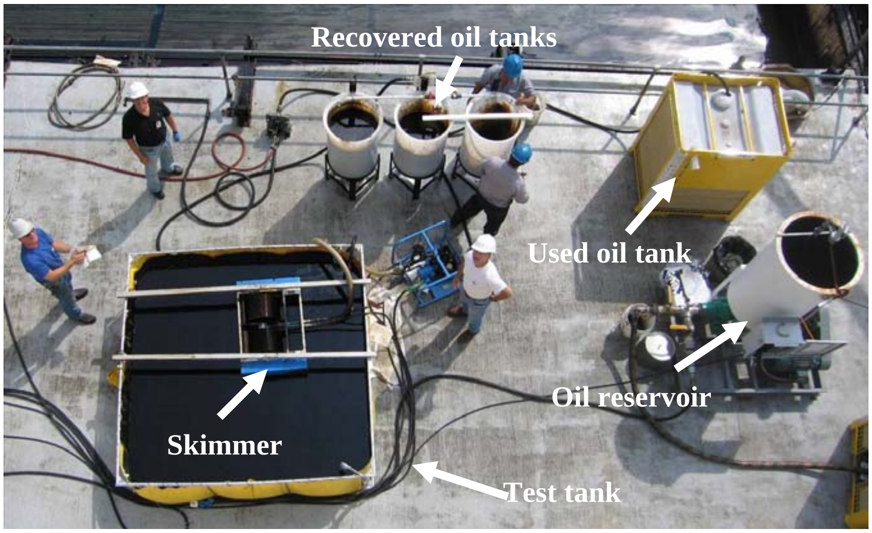


**Figure 12. Experimental setup at Ohmsett.**

### 3.2.2. Test Conditions and Variables

The following test conditions and variables were considered:

**Skimmer Design**: The Elastec/American Marine Mini-Max skimmer is an oleophilic rotating drum and frame skimmer. The unit recovers oil by cyclic rotational contact of the oleophilic drum surface with the oil slick. Oil that adheres to the surface is rotated with the drum out of the slick to be scraped-off by one or more wiper blades. Oil removed in this way collects in a trough and sump from which it is subsequently pumped out of the skimmer to mass storage. This type of skimmer is probably one of the simplest oleophilic skimmer designs. It is easy to handle, rig, and operate. Drum operation is straight forward, and drum changes are easily accomplished in the field. Therefore, for testing purposes drums made of different materials can be varied easily. Additionally, oil adhesion to the drum and drum rotation are easily observed and measured during testing.

As the test date approached, a new larger skimmer denominated Elastec TDS118G (PE-118) manufactured by Elastec/American Marine, with polyethylene grooved drums became available (Figure 13). Since this would be the commercial version of the new skimmer design, it was incorporated into the test protocol.

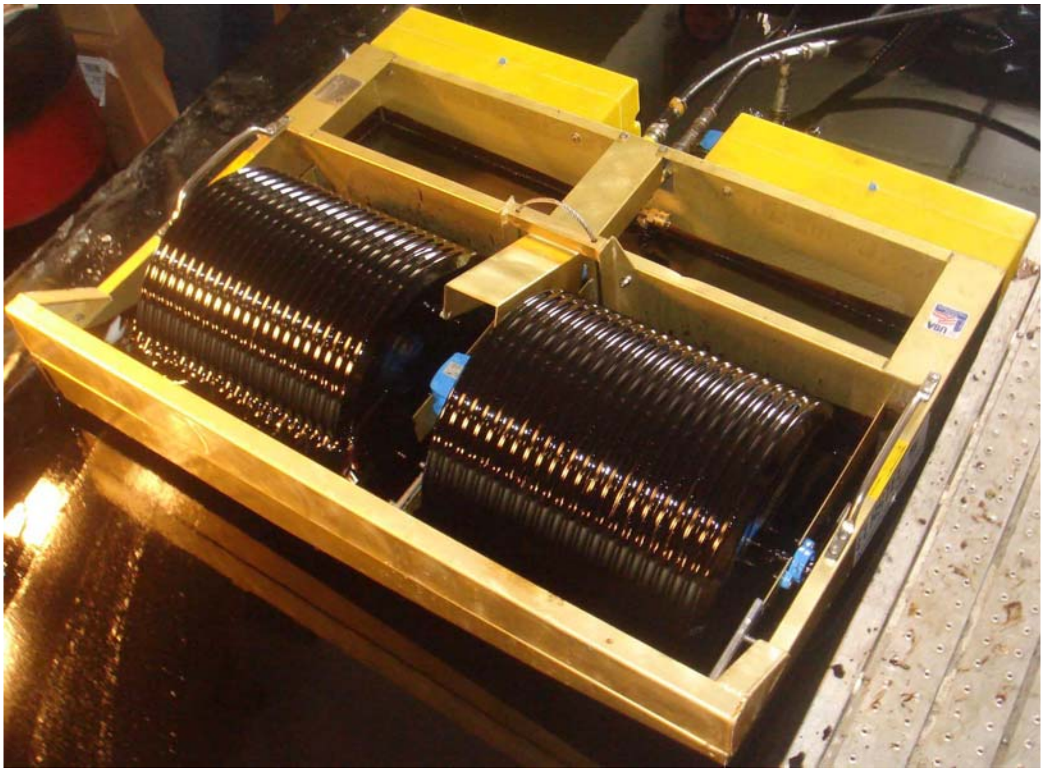

**Figure 13. PE-118 Skimmer with grooved drums**

**Oleophilic Drum Surfaces**: Based upon the laboratory studies, six surfaces with a combination of materials and surface patterns were considered. For the Mini-Max skimmer, three of the drums were made of aluminum with nominal $20^o$, $30^o$ and $40^o$ angles, and two additional drums at $30^o$ were coated with Neoprene and with Hypalon elastomeric surfaces. The actual dimensions of the grooved drums are presented in Appendix C; note that the actual angles differ considerably from the nominal. The grooved drum in the PE-118 was made of polyethylene.

**Skimmer Drum Speed of Rotation**: The speed of rotation of the oleophilic drum was held constant for each test, but was increased or decreases after each test to evaluate the effect of rotational speed on recovery efficiency. Although initially the drum recovers more oil with increasing speed, there is a maximum speed above which recovery does not increase or even begins to decrease as the oil film breaks apart due to the high rotational speed. The maximum speed was approximately determined for each oil by increasing the speed until the point where recovery did not increase. The typical rotational speeds varied from 10 to 60 revolutions per minute (rpm).

**Oil Type**: The same oils that were tested at Ohmsett were used, i.e. Endicott crude oil and HydroCal 300. We also tested diesel, which was also tested in the second test at Ohmsett. The oils were tested both fresh and mixed with slush ice. Oil properties (water content, viscosity etc.) were continuously monitored throughout the experiment.

**Oil Thickness**: A slick thickness in the range of 25 mm was maintained, as a defined test standard in the USCG regulations for determining Effective Daily Recovery Capacity (EDRC), and the ASTM F20.90 draft standard “Protocol for Measuring the Performance of Stationary Skimmers”. The 25mm thickness standard was chosen over the 10mm standard for its ease of maintenance during testing. The slick thickness was held within ± 5 mm, by adding sufficient oil after one or more tests to replace the oil recovered.

**Frazil Ice:** Several techniques were evaluated for making uniform ice shaving. A very sharp 8" auger was used to make the shavings from on fresh water ice. The ice shaving were flat, similar to frazil particle, but were very stable structurally. The dry shaving were harvested and stored in a cooler until they were used in the test.

**Other Parameters**: In addition to the variables previously listed, other variables were monitored and recorded. These include water bulk and surface temperature, oil bulk and surface temperature and air temperature. Additionally, oil distribution volumetric flow rate and pressure, and oil recovery volumetric flow rate and pressure will be recorded.

### 3.2.3. Post-field test sample analysis

Samples from the various oils were taken from their shipping container, from the test tank, and from the recovery tanks after each test. The oil samples were placed in 250 mL bottles and capped. The samples were shipped from CRREL to UCSB, where they were stored at – 4 $^{o}$C until they could be analyzed for water content and free water within the sample. The samples were in storage for an average of 4-6 weeks before analysis. The analyses were done at 22 $^{o}$C, allowing the samples to reach this temperature slowly.

Emulsified water was determined by Karl-Fischer titration, following ASTM D 4377-00, using a Mettler-Toledo (model DL 31, Figure 14) for the analysis. The sample size varied according to the estimated amount of water content in the oil sample. Appendix B presents the analytical procedures for determining free and emulsified water in these samples. The coefficient of variation for the Karl-Fischer titration was 1.97%. Free water was determined with an accuracy of ±0.5 mL, while the total volume of fluids (oil plus water) was determined to ±1 mL.

**Figure 14. Karl-Fischer titration apparatus.**

## 4. Results

Five different oils (three crude oils and two petroleum products) were studied in the laboratory, to understand the physicochemical behavior of oil and oil/ice mixtures in cold climates. In addition, a sample of weathered Endicott was also studied, since the properties of weathered crude oils are usually quite different from fresh crudes. Fresh Endicott crude oil was received from British Petroleum, via Alaska Clean Seas. A sample of this crude oil was sent to the UCSB laboratory after the field tests, since the properties of this oil were quite different from the weathered Endicott that had been tested before. The sample of weathered Endicott crude oil was received from Ohmsett in August 2006, before the field tests. HydroCal 300 was purchased from Calumet Lubricants. Diesel for the laboratory work was purchased in a local gasoline station in Goleta, CA. For the field tests, diesel was purchased from Irving Oil, a supplier in New Hampshire.

Seawater ice was used in all cases, shaved to a consistent length and shape. However, there is some natural variability in the consistency of the ice shavings, and the various oils behaved quite differently when ice was mixed in. For the more viscous oils (HydroCal 300 and weathered Endicott), the ice adhered strongly to the oil, forming a slushy mixture, which almost did not flow (Figure 15a). For the lighter crudes, particularly fresh Endicott, the ice would slowly tend to sink, separating from the oil (Fig.15b), although at high ice loading the mixture becomes cohesive (Fig. 15c). This was even more evident for diesel, where the ice would almost not mix with the oil, sinking to the bottom of the container (Fig. 15d). Thus, measuring the physicochemical properties of the oil/ice mixture became a significant challenge, and the values reported here represent the mean of a significant number of measurements, with some noticeable variability, as pointed out in the text.

(a) (b) (c) (d)

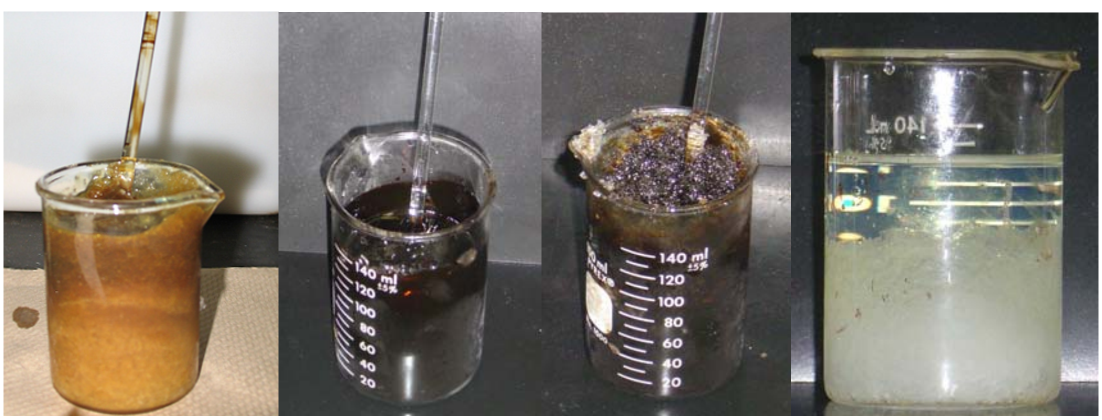

**Figure 15. a) HydroCal 300 and 60% ice mixture; b) fresh Endicott and 30% ice mixture; c) fresh Endicott and 80% ice mixture; d) diesel and 40% ice mixture.**

## 4.1 Physicochemical Properties of Oil and Oil/Ice Mixtures below freezing conditions

Three physicochemical oil properties are of most interest for oil recovery, namely oil density, viscosity and surface tension. The density of oil decreases linearly with increasing temperature (Figure 16), and thus can easily be predicted from knowledge of data at two temperatures or the equation of the line. Even weathered crude oil (Endicott) behaved very predictably. In general, the variation in density in this range is small, around -0.001 g/mL per $^{o}$C.

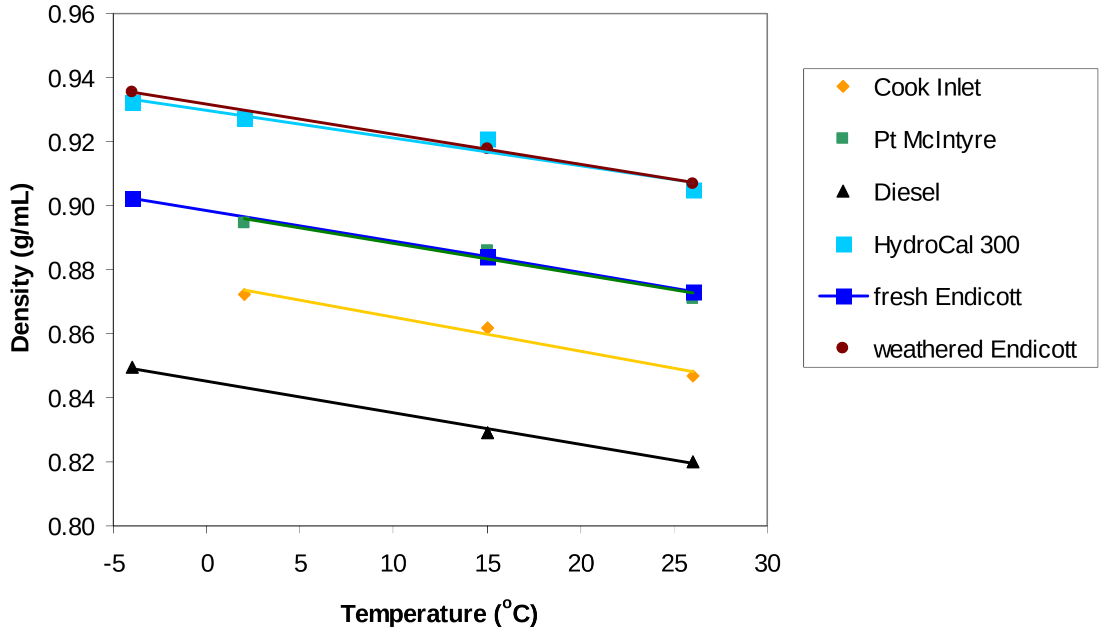


**Figure 16. Temperature dependence of oil density for various crude oils and petroleum products.**

Viscosity is a strong function of temperature and varies over several orders of magnitude in this range (Figure 17). Although in general a log-linear relationship can be used to predict the decrease in viscosity with increasing temperature, some of the more complex hydrocarbon mixtures deviate to some extent from this relationship.

Although the temperature dependence of each oil is linear with temperature, decreasing slightly with increasing temperature, each hydrocarbon mixture appears to have a different slope (Figure 18). The more homogeneous petroleum products appeared to have a similar behavior with increasing temperature.

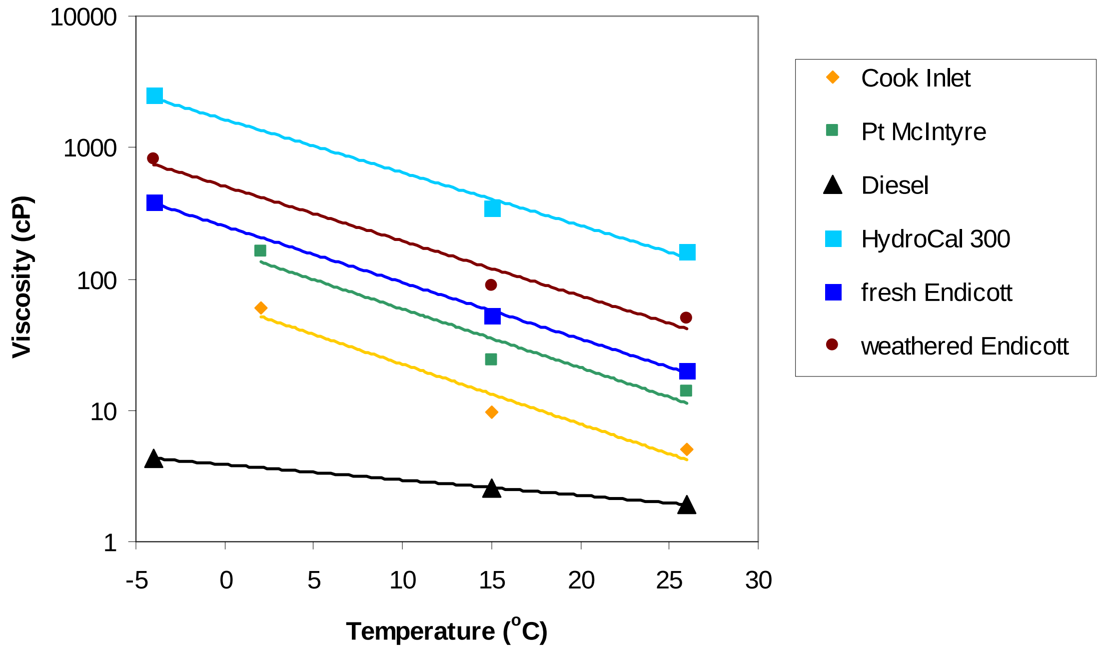


**Figure 17. Temperature dependence of oil viscosity for various crude oils and petroleum products. Note that the y-axis is logarithmic.**

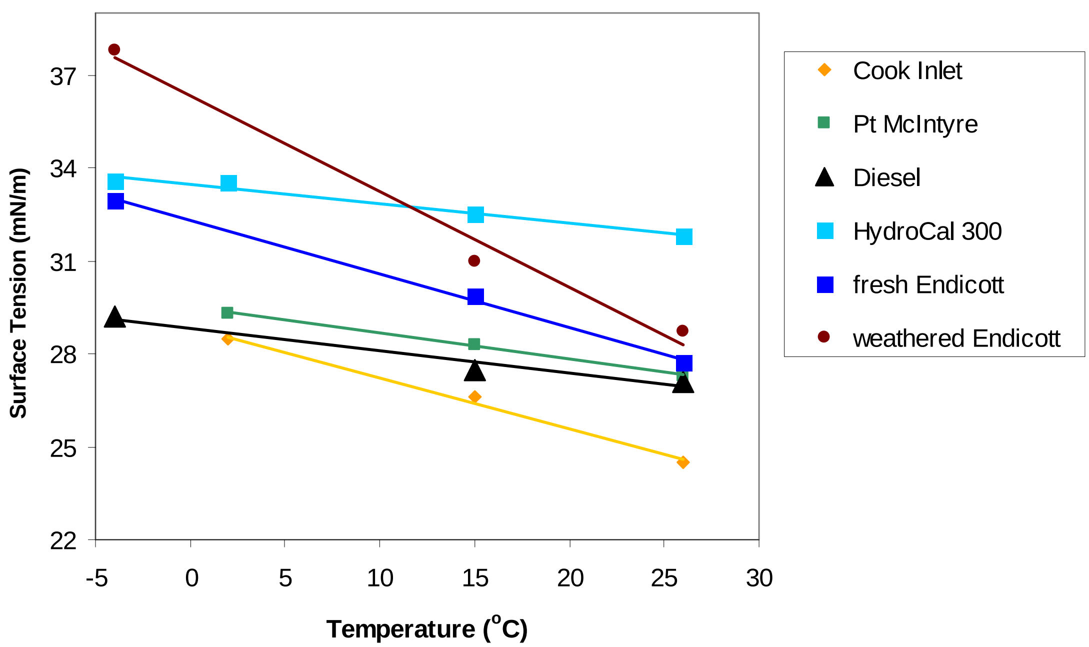


**Figure 18. Temperature dependence of surface tension for various crude oils and petroleum products.**

Studies of the behavior of oil/ice mixtures were conducted only with those oils that would be tested at CRREL, in part due to the limited amount of Cook Inlet and Point McIntyre crude oils.

Oil density varied noticeably with increasing ice content (Figure 19). Depending on whether the ice formed a more cohesive mixture with the particular oil or not, the density of the mixture either increased or decreased with increasing ice content. For example, HydroCal 300 and weathered Endicott formed a slushy oil/ice mixture, thus exhibiting a decreasing density with increasing ice content, particularly as the ice content increased beyond 20% by weight. The ice and Diesel or fresh Endicott mixtures increased in density with increasing ice content, although above 40% ice content, the fresh Endicott/ice mixture behaved like the more viscous oils. It is likely that viscosity plays a major role in the threshold point beyond which the mixture behaves more cohesively. As indicated before, the error in measurement of physicochemical properties increased with increasing ice content, due to the heterogeneous nature of these mixtures of solids and liquids, with different particle sizes for the ice. For example, Figure 19 presents error bars (± 1 standard deviation) for fresh Endicott for 40 and 60% ice content. Note that the general trend (increasing and then decreasing) still holds. Other error bars not shown for clarity. It should be noted that these oil/ice mixtures were much better mixed than the mixtures used in the field tests, and in fact would not directly reflect the likely mixture in a real oil spill in ice, but they serve to understand the behavior of ice (i.e. whether it forms cohesive mixtures or not), and the potential effect on density.

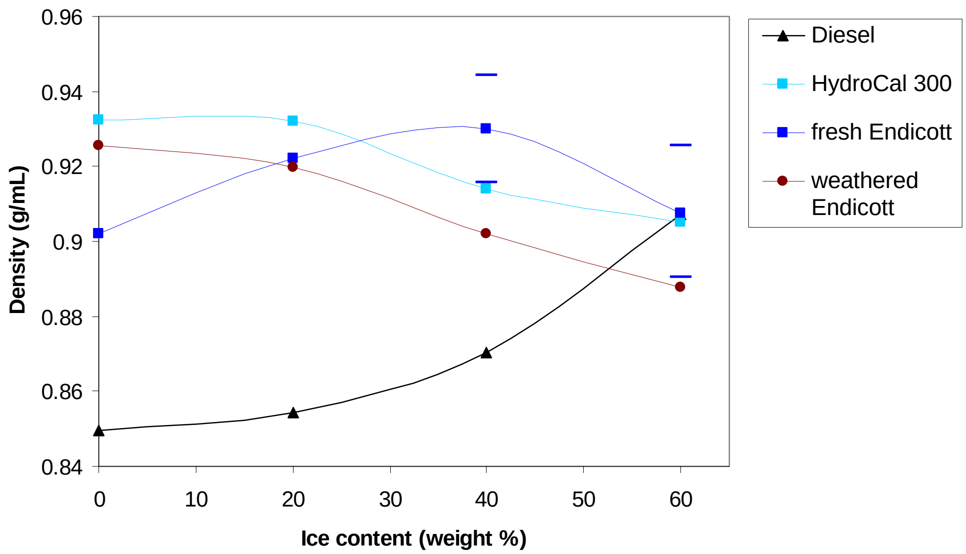


**Figure 19. Behavior of oil density with increasing ice content. Fresh Endicott values with ± 1 standard deviation shown for 40 and 60% ice content.**

The viscosity of HydroCal 300 increased quite significantly with increasing ice content (Figure 20). Given the high initial viscosity of HydroCal, it tends to adhere to the ice particles and coat them, creating an increasingly more viscous mixture. The behavior can best be fitted with a quadratic equation, although the physical basis for such a relationship is unclear. Since the mixtures of HydroCal and ice were relatively cohesive, the error bars (± 1 standard deviation) are small, although there is increasing heterogeneity with increasing ice content.

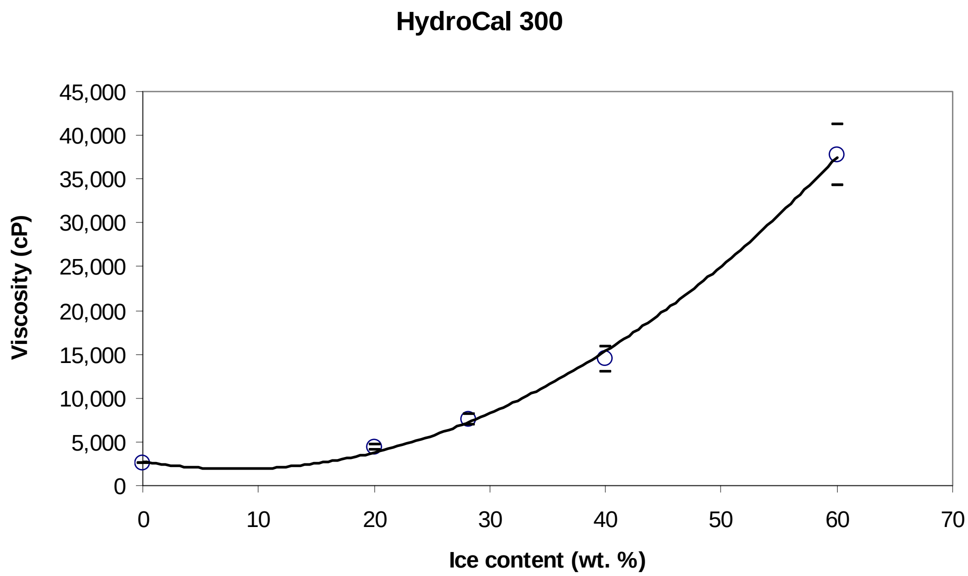


**Figure 20. Behavior of HydroCal's viscosity with increasing ice content.**

Since Endicott is a relative light crude, it tends to separate easily from the ice particles. However, there is a significant increase in viscosity as ice is mixed in (Fig. 21). It is also important to note that since the viscosity of the oil increases rapidly as temperature decreases even just a few degrees, the behavior of the oil/ice mixture can be very different, as can be seen in the much higher increase in viscosity at – 5 $^{o}$C.

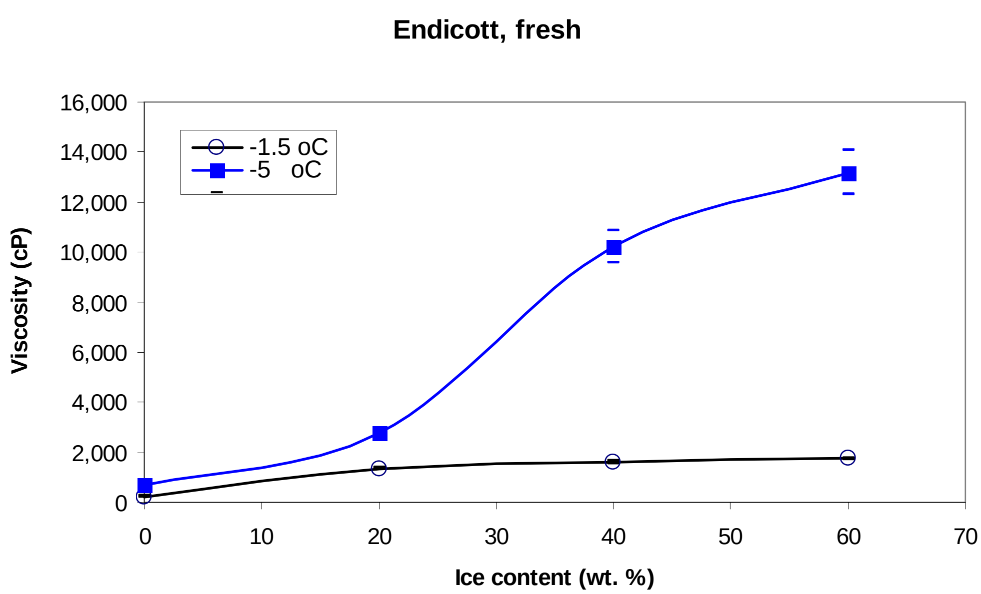


**Figure 21. Behavior of fresh Endicott's viscosity with increasing ice content.**

The viscosity of weathered Endicott behaved quite differently, starting from a very high viscosity and then decreasing with increasing ice content until around 40% ice by weight. At that point, the viscosity of the mixture seemed to remain relatively constant at around 15,000 cP even as the ice content increased to 60% (Figure 22).

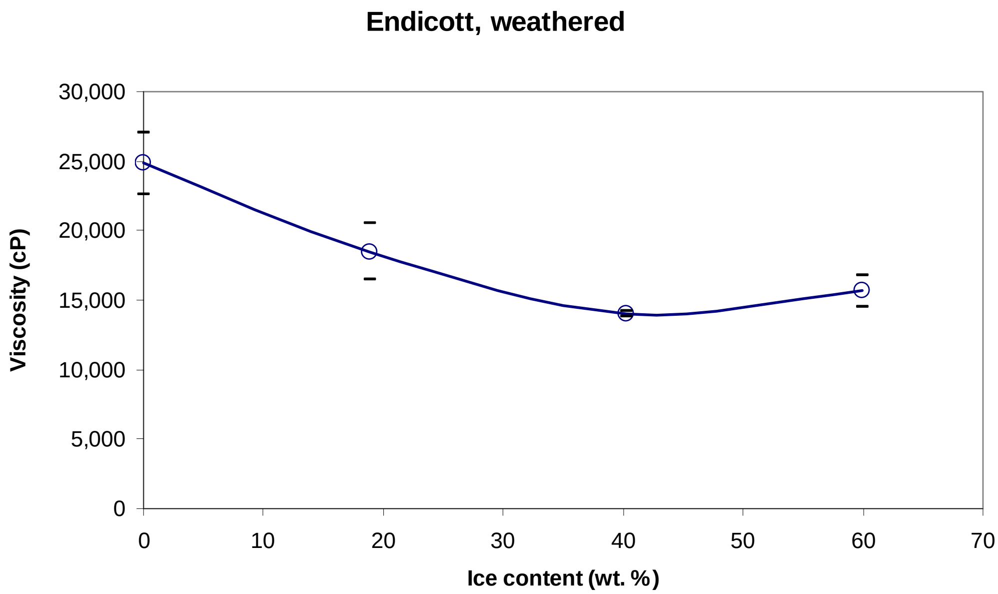


**Figure 22. Behavior of weathered Endicott's viscosity with increasing ice content.**

In the case of diesel, the viscosity increased considerably with increasing ice content, and did so monotonically. Given the fact that the diesel/ice mixtures don't form a cohesive mixture, the error bars in the measurement of the viscosity of the mixture are quite large, as shown in Figure 23.

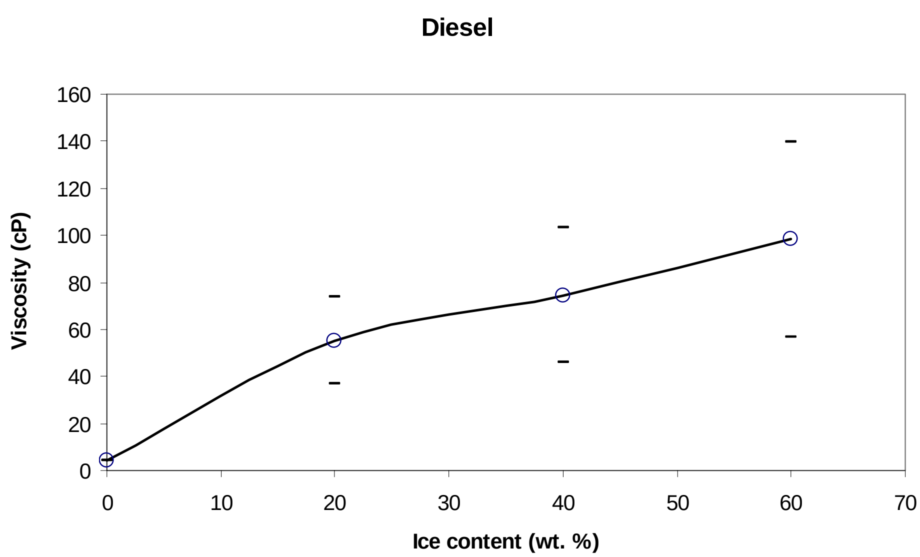


**Figure 23. Behavior of diesel's viscosity with increasing ice content.**

Although the addition of ice does affect the surface tension of the oils, the changes were relatively small, and the direction of the changes was not easy to predict. For example, the surface tension of HydroCal 300 and ice mixture increases slightly as the ice content increases from 0 to 60% (Figure 24).

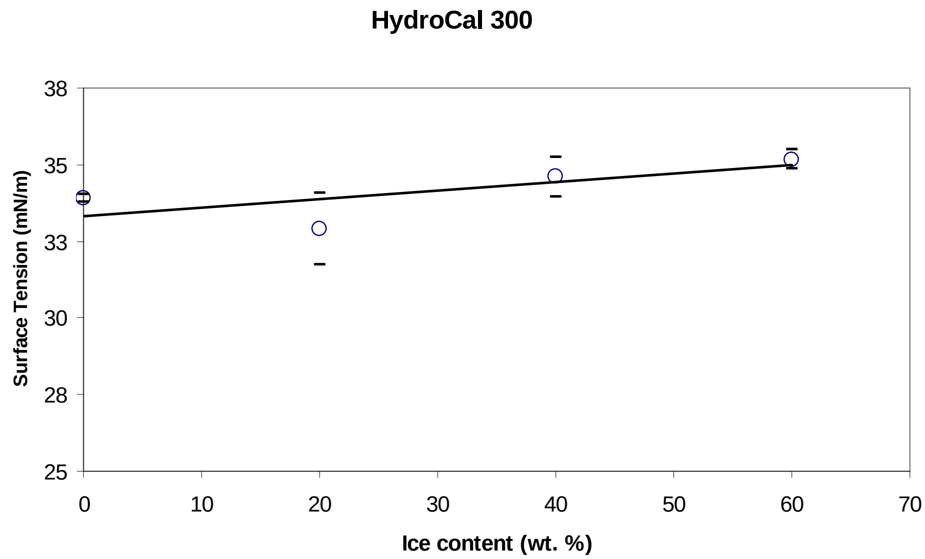


**Figure 24. Behavior of HydroCal's surface tension with increasing ice content.**

For Endicott, the change was also relatively small. In fact, for fresh Endicott the effect on surface tension was minimal (Figure 25); it was more significant for weathered Endicott.

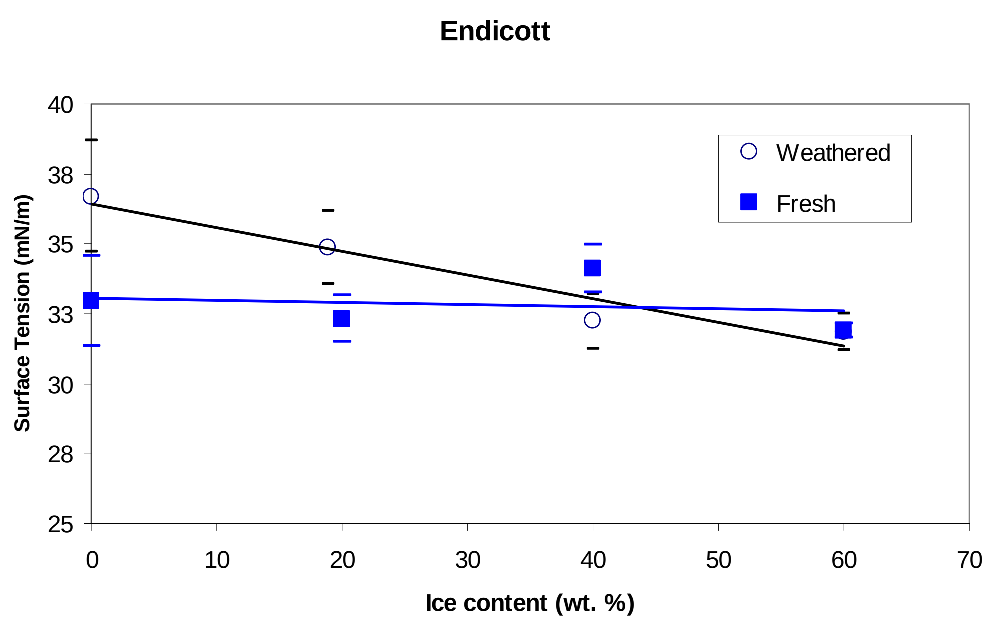


**Figure 25. Behavior of Endicott's surface tension with increasing ice content.**

Similar to fresh Endicott, the effect of increasing ice content was very small for diesel (Fig. 26). Since the ice tends to sink below the oil surface, it does not have a noticeable effect on surface tension.

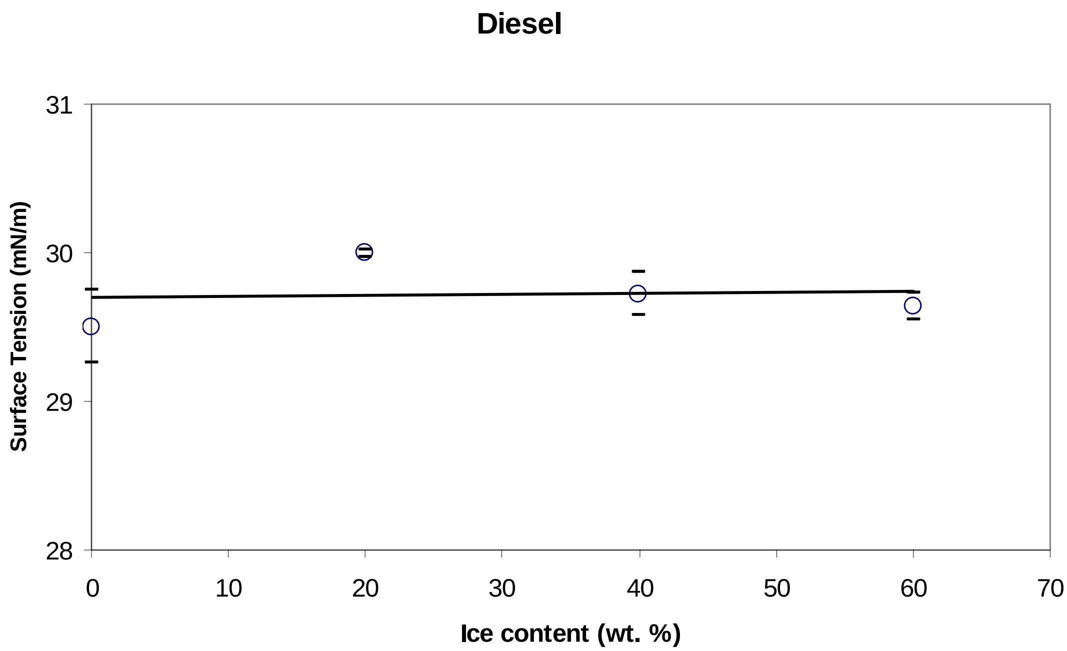


**Figure 26. Behavior of diesel's surface tension with increasing ice content.**

Overall, the mixing of oil and ice has the most significant effect on viscosity. While in most cases the viscosity of the mixture increases, in the case of weathered Endicott, which was very viscous to begin with, the effect was the opposite. It appears that the effect of mixing oil and ice is most significant when the oil and ice form a cohesive mixture (e.g. HydroCal 300), and would be less important for light oils which tend not to form cohesive mixtures with ice (e.g. diesel and fresh Endicott).

### 4.2 Recovery of Oil and Oil/Ice Mixtures below freezing conditions

Although it is useful to understand the behavior of basic physicochemical properties, one of the most relevant questions for oil recovery is how much does oil spilled on a waterbody adhere to an oil recovery surface, such as a skimming drum. It is also important to understand the effect of ice content on recovery. Although a number of additional materials were tested (e.g. Polyurethane, Teflon), in this report the results of the tests with the most promising materials are presented. They were: Neoprene, Hypalon, Styrene-Butadiene Rubber (SBR), Low Density Polyethylene (LDPE) and Aluminum (Al).

In Figure 27, the difference in mass of HydroCal 300 recovered between different materials indicates that Neoprene would be the best recovery surface, for ice contents from 0 to around 60%. The rest of the materials fall closely together in terms of adhesion of oil (i.e. mass recovered) to the surface. There is considerable variability in the measurements, particularly as the ice content increases. For ice content up to 20%, the normalized mass recovery has a coefficient of variation (standard deviation/mean) of 6-12%, while for higher ice content the coefficient of variation is up to 30%.

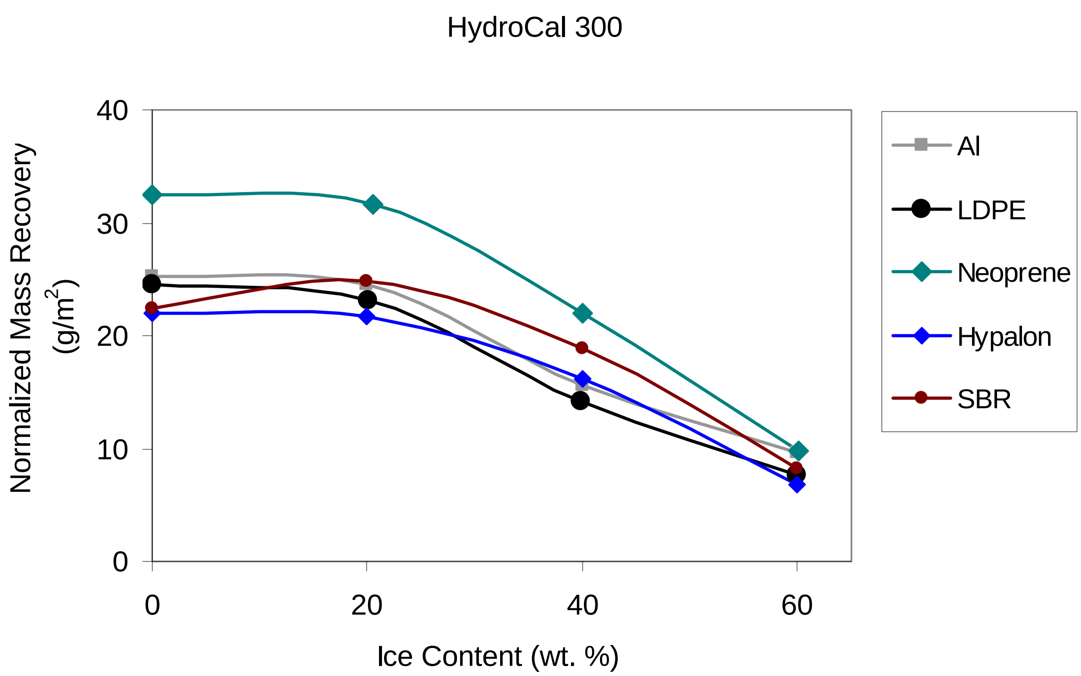


**Figure 27. Effect of increasing ice content in HydroCal 300 on oil recovery.**

Higher recovery (i.e. higher adhesion to the surface) correlates well with a lower dynamic advancing contact angle, as shown in Figure 28, at least for HydroCal 300. However, even though the dynamic advancing contact angle drops substantially for LDPE at 60% ice content, it does not seem to improve its ability to recover more oil from the surface (Fig. 27). The coefficient of variation ranged from 1-7.4% at low ice content, up to 33% for ice content above 20%.

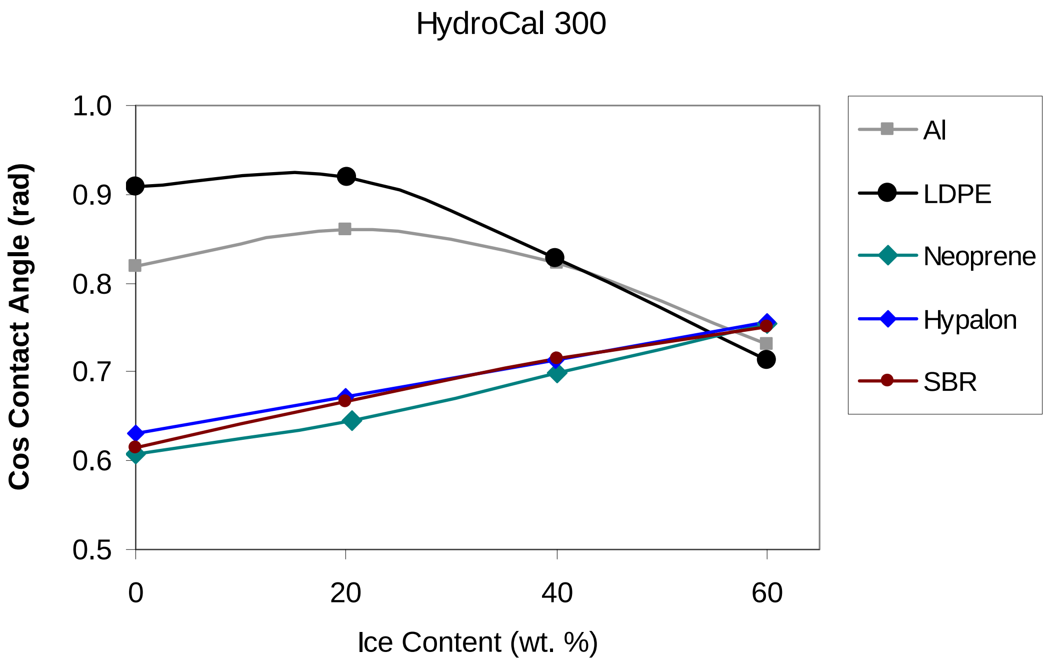


**Figure 28. Effect of increasing ice content in HydroCal 300 on the dynamic advancing contact angle.**

Although Hypalon appeared to be a better surface for recovering fresh Endicott when only oil is present, with increasing ice content Neoprene becomes the best surface, for those materials tested (Figure 29). In general the elastomeric materials (Neoprene, Hypalon and SBR) performed better than the hard plastic (LDPE) or the metal (Aluminum) surfaces. The Hydrophobicity and porosity of these surfaces increases the adhesion of hydrocarbon liquids. The dynamic advancing contact angles appear not to be good predictors of adhesion (Fig. 30), since it is not always clear that the most wetting condition will result in higher oil recovery. Overall, some of the highest mass recoveries were observed for fresh Endicott. The range of coefficients of variation was similar for normalized mass recovery and dynamic advancing contact angles as for HydroCal 300.

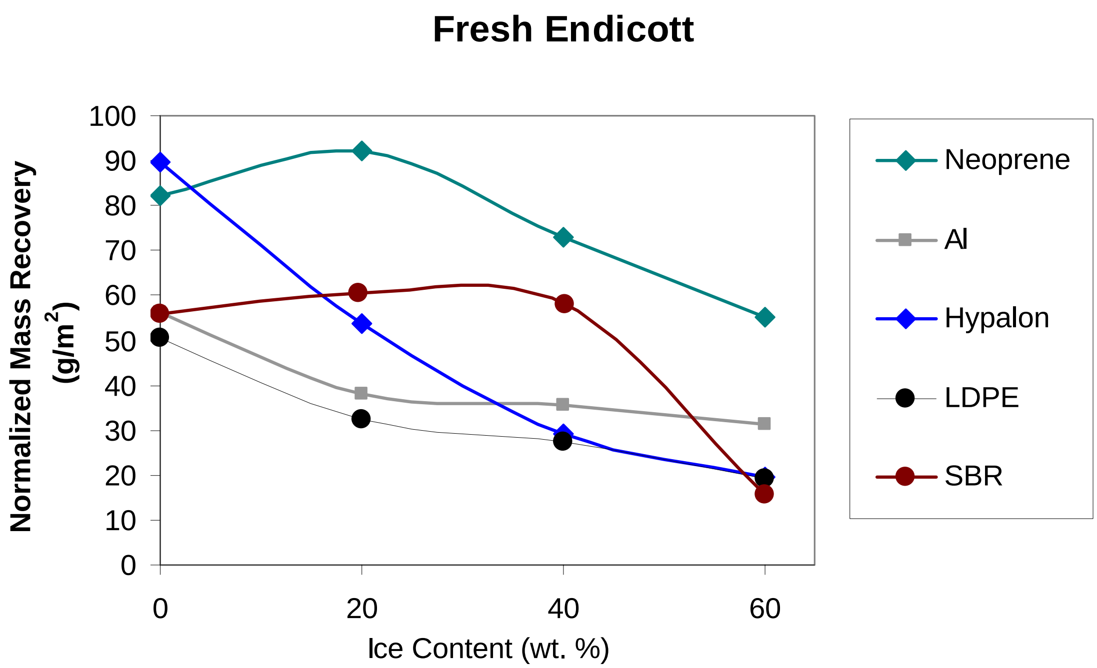


**Figure 29. Effect of increasing ice content in fresh Endicott on oil recovery.**

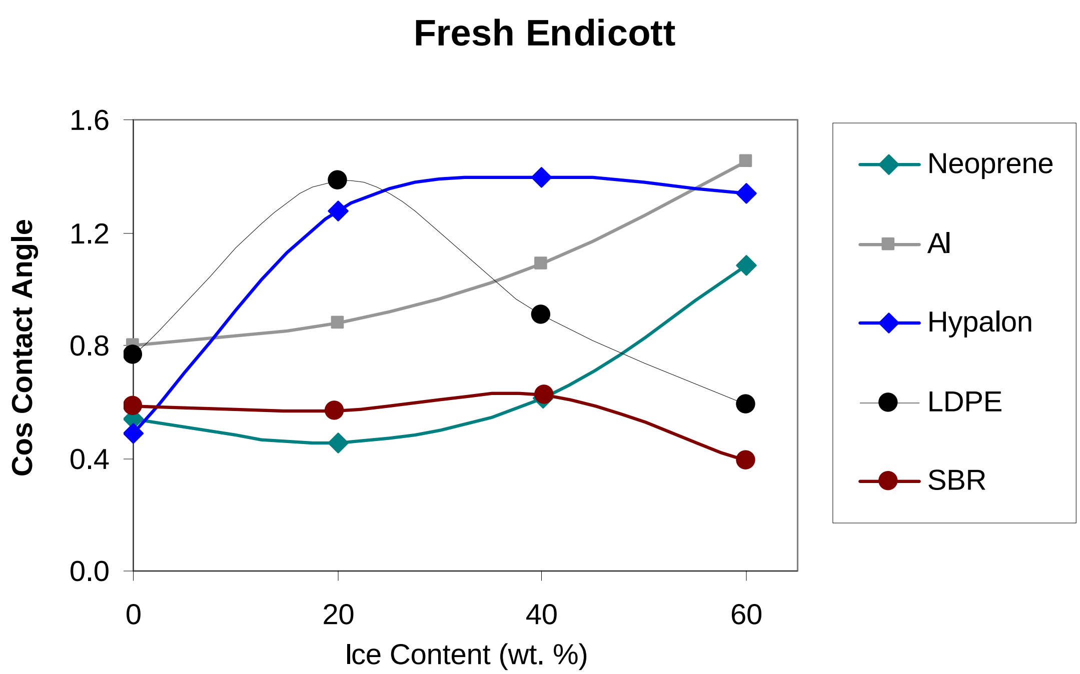


**Figure 30. Effect of increasing ice content in fresh Endicott on the dynamic advancing contact angle.**

In the case of diesel, Neoprene was almost in all cases the preferred surface (Figure 31). Overall, the mass recovery of diesel was the lowest, in part due to its lower viscosity. The dynamic advancing contact angle remained fairly constant even as the ice content of the mixture was increased to 60%, for all materials (Figure 32).

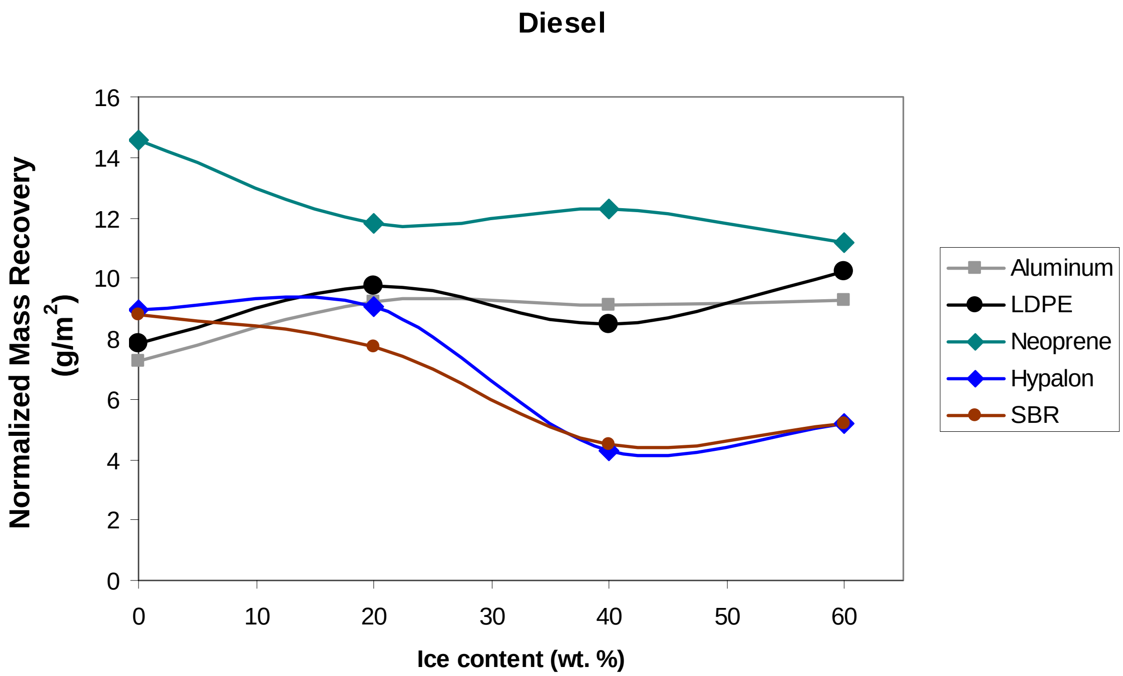


**Figure 31. Effect of increasing ice content in diesel on oil recovery.**

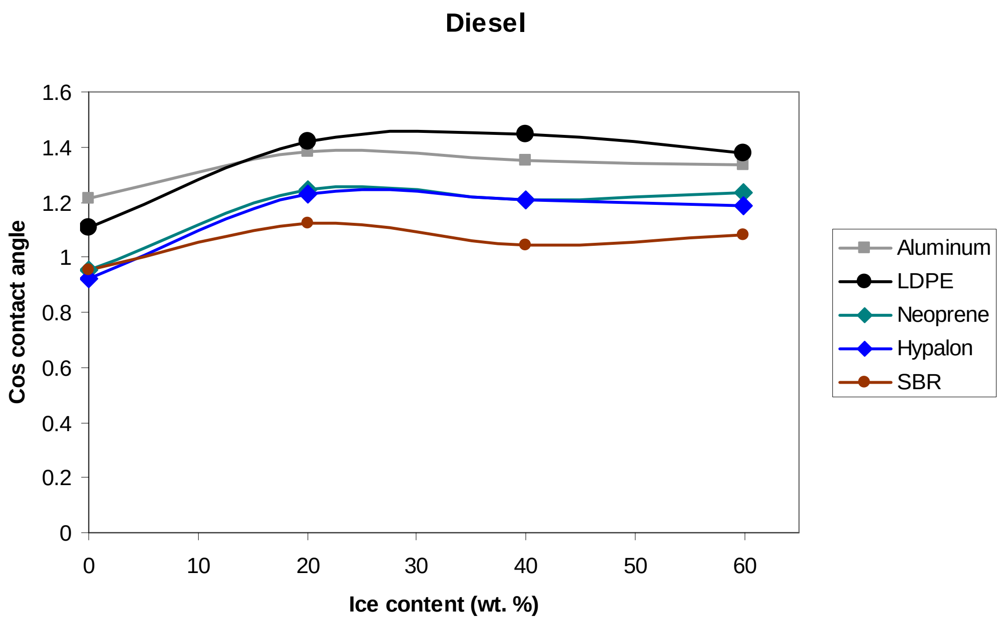


**Figure 32. Effect of increasing ice content in diesel on dynamic advancing contact angle.**

The results from these laboratory experiments indicated that recovery of the various oils would be feasible in these cold climate conditions, but that the increase in viscosity both due to the low temperatures and the presence of ice could have an impact on the performance of the skimmer. It also became clear that a Neoprene coated drum should be tested in the field, along with the available aluminum and LDPE drums.

### 4.3 Field tests at CRREL

A total of 94 tests were conducted at the MEF in CRREL in six working days. Two additional days were used for initial test setup and debugging of pump and skimmer issues at these cold temperatures, one day was used for cleaning the entire system, and one day was used for shipping the equipment back to Ohmsett. The three oils were tested, with and without ice, for most of the drum surfaces. The full test results are available in Appendix A. Due to time and budget constraints, conducting replicates of every test was not feasible. However, duplicates of some tests were conducted. The results of these duplicates indicate the oil recovery rates are within ± 5 to 10%. For clarity, error bars are not included in the following charts, but it should be understood that these values are within this margin of error.

#### 4.3.1 HydroCal tests

The HydroCal tests were conducted first, since Endicott tends to leave a significant residual and it was important not to affect the conditions of the various tests. Endicott was tested second, since diesel is a good solvent for Endicott and thus it is best to use it last, removing any Endicott residual from the tank with minimal change in properties. After testing each oil pumped directly from the shipping vessels to the system, tests were conducted with ice, with approximately 30% ice content by mass. The necessary ice to achieve 30% ice content was estimated based on the known amount of oil in the test tank and the density of the ice. The ice was added in a volumetric basis (Figure 33). The amount of ice in each ice chest was determined using a measured density of 482 $kg/m^3$ for the ice shavings, plus careful weighing of the ice chest before and after each load of ice was added, to ensure that the amount of ice added was adequate.

**Figure 33. Addition of ice to the oil (HydroCal 300) in the test tank.**

From the initial runs with HydroCal at -1.1 $^{o}$C (water temperature), without ice, it became clear that the rotational speed of the drum would have to be below 30 rpm, since the viscosity of HydroCal at this temperature was above 1,000 cP, and rotating at a faster rate would break up the 25 mm oil film, entraining too much water. Even at this rotational speed, the grooves in the drum were full (Figure 34), such that rotating the drum at a higher speed would not recover additional oil.

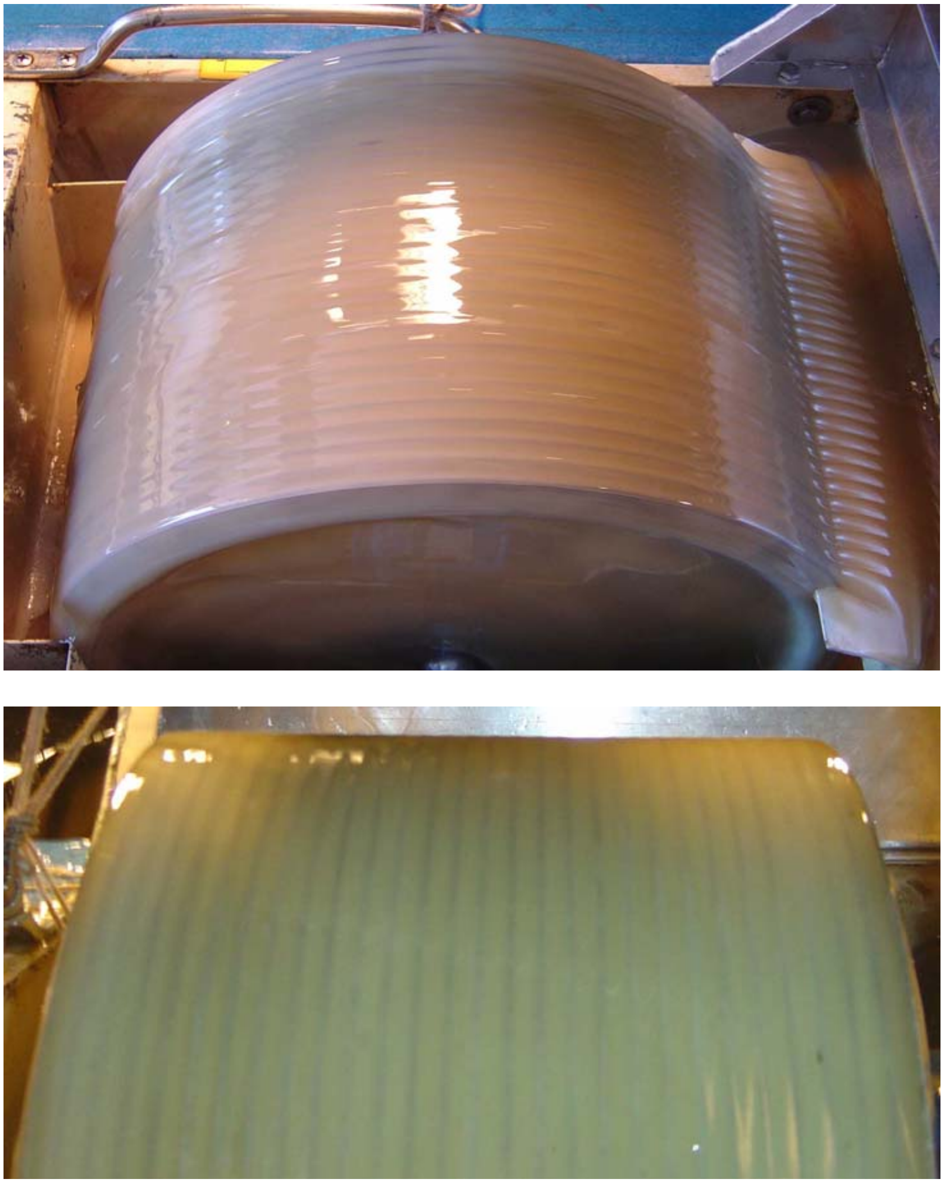

**Figure 34. Mini Max grooved drum recovering HydroCal 300 at -2 $^{o}$C, (a) side view; (b) frontal view.**

As can be seen in Figure 35, oil recovery rate was essentially the same at 20 and 30 rpm. These recovery rates are for one drum only, and would be doubled if both drums recovered oil. Thus, to determine the performance of the skimmer at different rotational speeds, tests were conducted at 10, 15 and 20 rpm. In general it was found that the recovery rate for HydroCal was insensitive to the material of the drum surface and groove geometry at low rpm, and that it was only at 20 rpm that a significant difference was observed between the different groove angles, with the 30$^{o}$ groove performing best and the 20$^{o}$ groove recovering significantly less. It should be noted that the cleaning blades for the 20$^{o}$ and 40$^{o}$ grooves had not been adjusted to the drums before shipment to

CRREL, and that personnel from Elastec/American Marine performed the adjustment on-site, resulting in some mismatch between the geometry of the cleaning blade and the drum grooves. From previous work, we would expect that the wider ($40^o$) grooves would be better for recovering more viscous oil such as cold HydroCal. All the grooved drums significantly outperformed the flat drum (Fig. 36), particularly as the drum speed increased. The PE 118 drum was not used in these tests.

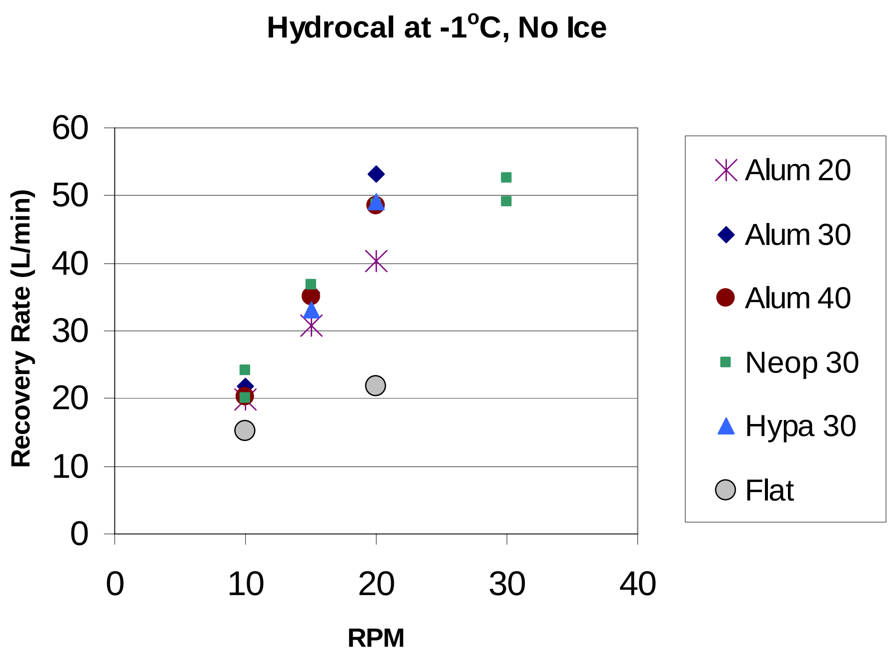


**Figure 35. Recovery rates for HydroCal at -1 $^o$C, without ice, after subtracting any free or emulsified water. Data for one drum recovering oil. Note: 10 L/min = 2.64 gal/min, 10 gal/min = 37.85 L/min.**

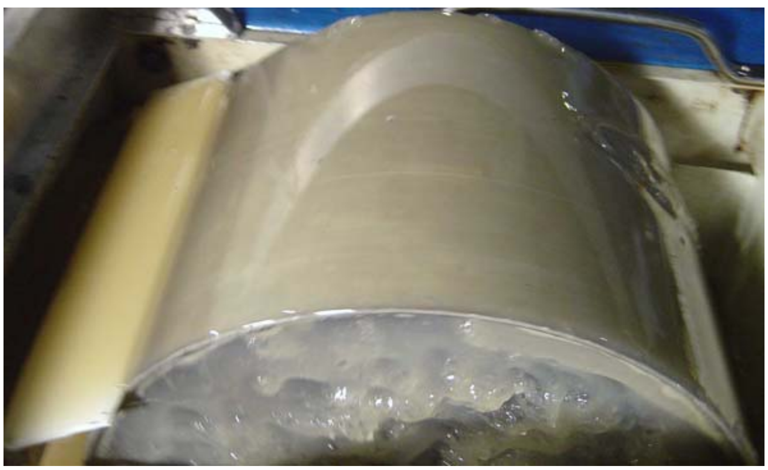

**Figure 36. Flat drum recovering HydroCal at 20 rpm.**

Although the data presented in Figure 35 reflects only oil recovery, after subtracting any free or emulsified water, it would be almost the same if the free or emulsified water was considered, since the actual amount of free water was almost nil in all cases and significantly less than 1% emulsified water, since care was taken to minimize emulsification. For example, instead of recirculation the oil while the drum speed was adjusted, instead the cleaning blade was lifted while the drum speed was adjusted. Thus, most of the oil recovered was free of water. HydroCal did form a light foam (oil/air mixture) as the HydroCal rotated on the drums (Figure 37).

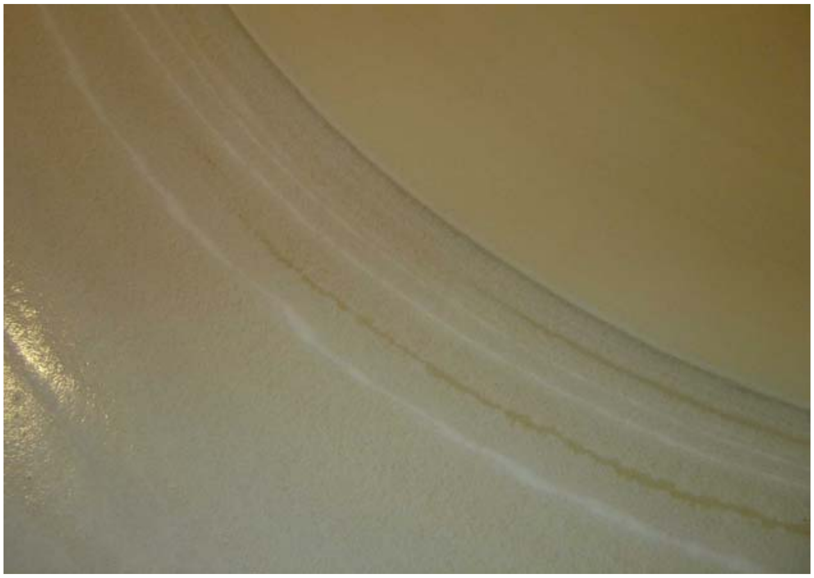

**Figure 37. HydroCal foam in the test tank.**

Once shaved ice (Figure 38) was added to HydroCal in the test tank, it was mixed in manually using a paddle, in a slow circular motion to avoid emulsifying the oil (Figure 39). The resulting mixture appeared fairly homogeneous, although it is possible that some ice clusters remained.

**Figure 38. Consistency of shaved ice used at CRREL.**

**Figure 39. Mixing of ice with HydroCal 300 in circular motion.**

As the drum was rotated, it became clear that ice would be lifted out of the surface along with HydroCal (Figure 40). No accumulation of ice was seen at the point where HydroCal was lifted by the drum throughout the tests. Even when some ice clusters approached the skimmer, they were either lifted out of the surface or they went past the skimming drum.

**Figure 40. Ice lifted out of the oil/ice mixture along with HydroCal 300.**

As expected, the HydroCal/ice mixture did not emulsify, maintaining a low water content in the HydroCal (much less than 1%). However, since ice clusters were lifted along with the oil, the free water content, once the ice melted, was between 2 and 13%. Note that the recovery rate is linear with respect to rpm at this range of speeds. The recovery rates presented in (Figure 41) are after subtracting free and emulsified water. Under these conditions, the 30$^{o}$ drum and the PE 118 skimmer performed significantly better than the other groove angles (20$^{o}$ and 40$^{o}$) and the flat drums. Due to time constraints, the Neoprene and Hypalon drums were not tested, since it was apparent that their performance would not be significantly different than for the 30o aluminum drum. The 40$^{o}$ drum and the PE 118 were the most influenced by the amount of ice recovered along with HydroCal, since wider grooves can lift bigger pieces of ice than the narrower 20$^{o}$ and 30$^{o}$ grooves.

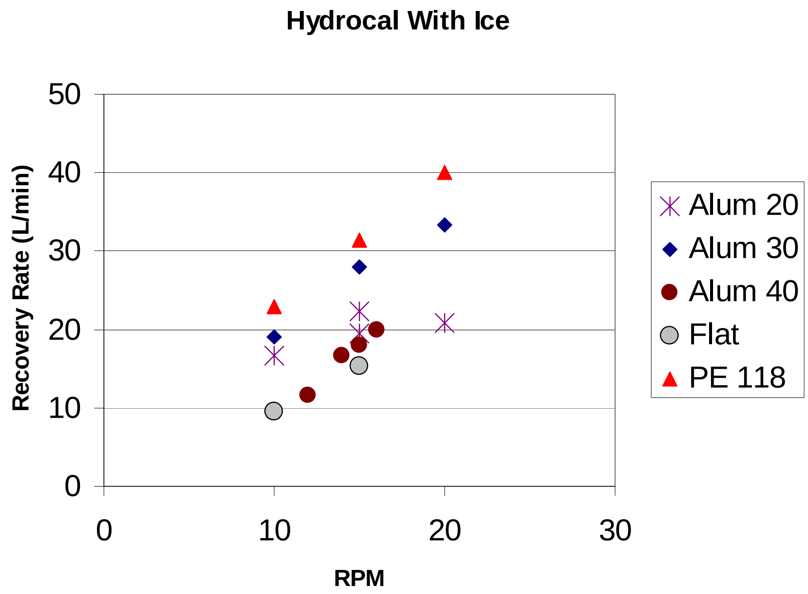


**Figure 41. HydroCal recovery rates at -1 °C when ice is present at 30% by weight. Recovery rate after subtracting any free or emulsified water. Data for one drum recovering oil.**

Although the skimmer performed remarkably well in the presence of ice, both for grooved and flat drums, there was a significant difference in recovery rates. The presence of ice decreased HydroCal recovery rates considerably, particularly at higher rpm (Figure 42). At 10 rpm, the decrease was around 12 to 15%. At 20 rpm, the decrease was on the order of 40 to 50%.

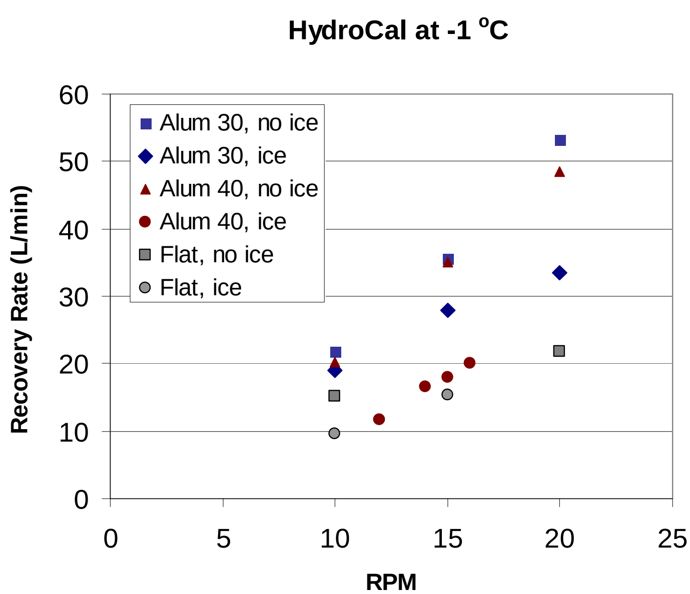


**Figure 42. Comparison in recovery rates for HydroCal at -1 °C, in the absence and presence of ice. Recovery rate after subtracting any free or emulsified water. Data for one drum recovering oil.**

### 4.3.2 Endicott tests

The Endicott received was a relatively fresh oil, with an average viscosity at 0 °C of around 300 cP. After HydroCal was removed to leave only a light sheen of oil and no ice in the tank, a sufficient amount of Endicott was pumped into the test tank to obtain a 30 mm thick oil layer. Rather than start at 25 mm and risk having a very thin oil layer, the tests were run from 30 to 20 mm, with an average 25 mm thickness. Within this range, the effect of oil layer thickness is minimal, as shown in our previous experiments at Ohmsett. The same procedure was used to minimize emulsification, namely avoiding recirculation of the oil by lifting the cleaning blade off the drums. However, the final analysis did indicate that there was around 1.3 to 3.9% free water and 0.2 to 1.1% emulsified water in the final results. It appears that a fraction of this water was already in the original oil, and that it simply separated during storage and warming up to room temperature for the analysis, since the samples taken from the recovery tanks did not appear to have any water.

The recovery rate of Endicott oil under freezing conditions but without ice is presented in (Figure 43). All the grooved drums significantly outperformed the flat drum. At the higher rpm, the grooves were almost full of Endicott, indicating a very successful recovery (Figure 44). The Hypalon drum could not be used for further tests since there was some damage in one of the grooves which was damaging the cleaning blade and was resulting in an inaccurate measurement of its performance. Given its larger capacity, the PE 118 system was able to recover substantially more oil than the smaller Mini Max drums, and it was able to recover oil even at 63 rpm, while the Mini Max drums seemed to reach a maximum closer to 50 rpm. As observed with HydroCal, the recovery rates for Endicott were not very sensitive to groove angle or material on the surface, with about the same recovery rate for all grooved Mini Max drums; the grooved drums did recover significantly more than the flat drum.

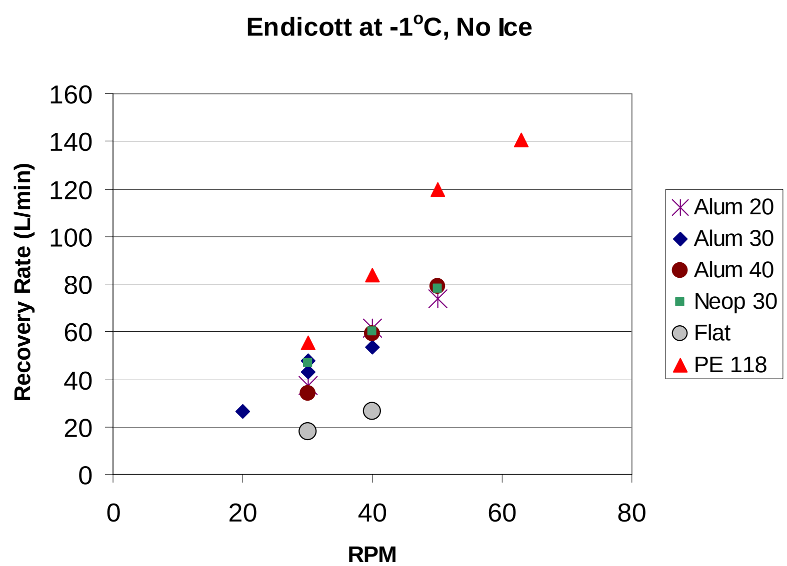


**Figure 43. Recovery rates for Endicott at -1 °C, in the absence of ice. Recovery rate after subtracting any free or emulsified water. Data for one drum recovering oil.**

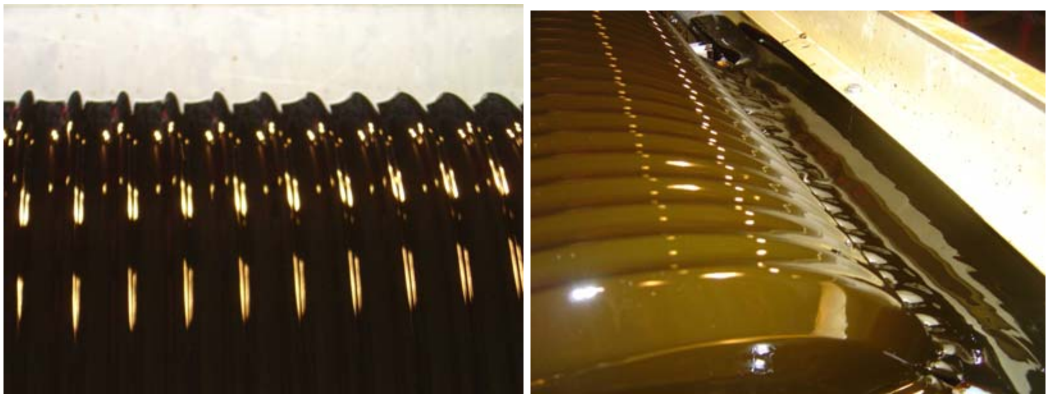

**Figure 44. Grooves filled with Endicott oil, for a drum speed of 50 rpm.**

After adding ice to around 30% by weight, the recovery rates for Endicott were measured (Figure 45). The ice tended to sink below the Endicott, so it was actually difficult to determine whether there was indeed ice, but samples taken from different points indicated that mixing was successful in minimizing large ice clusters. The large PE 118 drum reached a maximum recovery rate at around 40 rpm, beyond which too much ice was being lifted and the recovery rate was not increasing, since the grooves were already full. The Mini Max drums seemed to also reach a maximum recovery rate at around 40 rpm, beyond which the recovery rate actually decreased since the oil layer began to break up. Below 40 rpm, the recovery rates were practically linear with drum rotational speed for the Mini Max drums, flat or grooved. Under these conditions, the narrower 20$^o$ and 30$^o$ grooved drums performed better than the 40$^o$ drum. All grooved drums recovered more oil per unit time than the flat drum. Due to time constraints, the Neoprene drum was not tested under these conditions. Similar to the experience with HydroCal, no significant amount of ice was seen to build up near the recovery point (Figure 46).

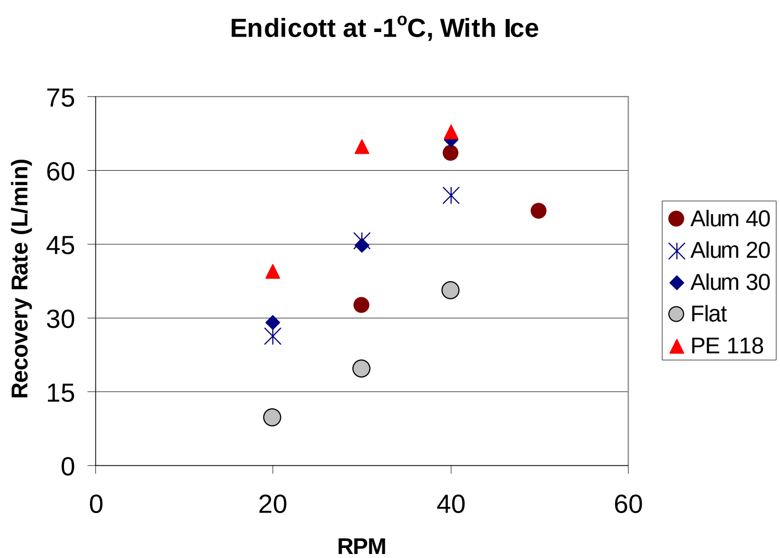


**Figure 45. Recovery rates for Endicott at -1 $^o$C with ice present at 30% by weight. Recovery rate after subtracting any free or emulsified water. Data for one drum recovering oil.**

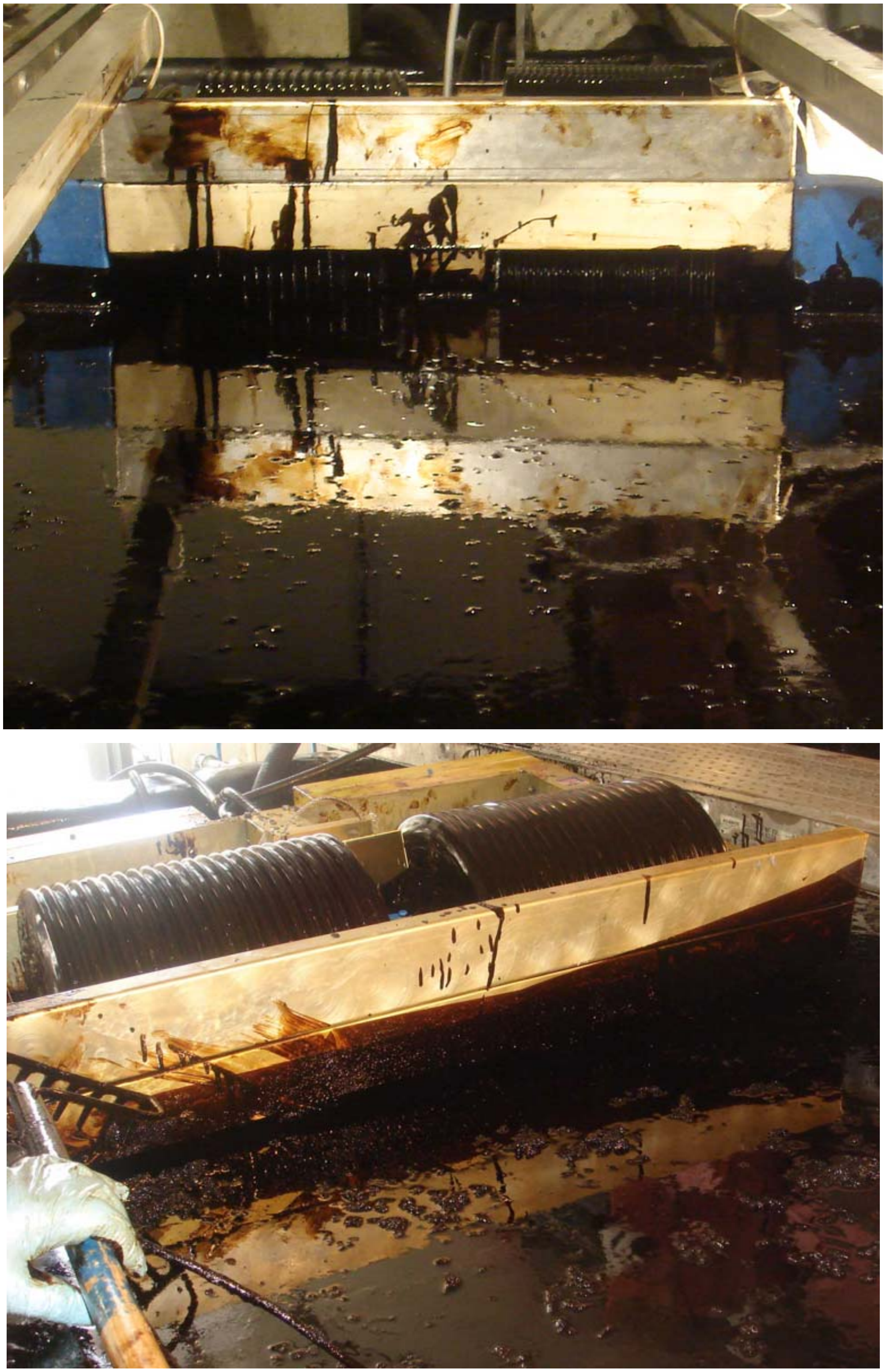

**Figure 46. Minimal ice buildup behind (a) Mini Max skimmer and (b) PE 118 skimmer.**

Although the two systems (Mini Max and PE 118) performed very satisfactorily with ice, in some cases there was a decrease in recovery rate due to the presence of ice. To a significant extent this was due to the ice recovered along with the Endicott oil, which was mixed in with the oil as it passed through the recovery pump. The emulsified water for these tests was in the range from 4.7% to 15.1%, and the free water was 4.0% to 21.4%. The decrease was most significant for the PE 118 drum at high rpm, and was less important for the grooved drums, once free and emulsified water are subtracted from the overall recovery rate. In fact, at 20 rpm, there was practically no difference between recovery in the presence or absence of ice, for all drums (Figure 47).

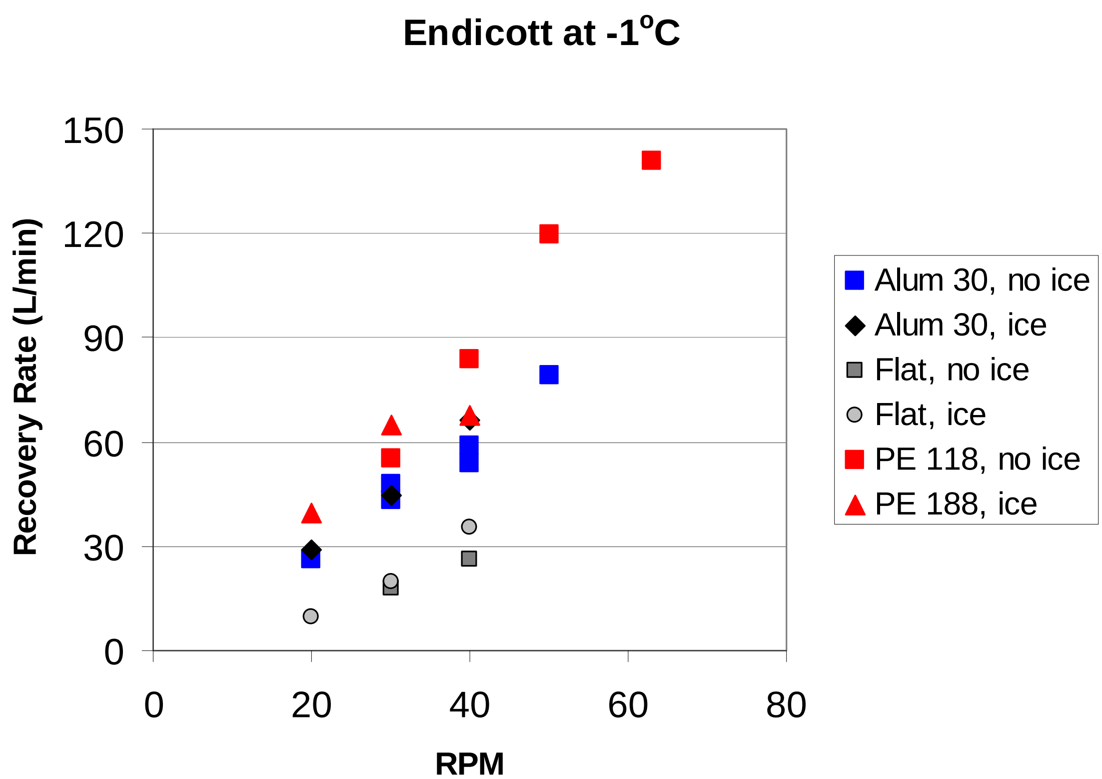


**Figure 47. Comparison in recovery rates for Endicott at -1 °C, in the absence and presence of ice. Recovery rate after subtracting any free or emulsified water. Data for one drum recovering oil.**

### 4.3.3 Diesel tests

After the Endicott with ice tests were completed, the skimmers were used to recover all the oil in the test tank. It was observed that recovery was high up until the point where the oil began to break up into disconnected regions. At that point, the skimmer rotational speed had to be reduced to 20 and then 10 rpm, to reduce the amount of water recovered, and the oil had to be boomed in to maintain a thicker layer. Some of the residual oil was recovered using adsorbent pads. Since there was a significant amount of ice left in the test tank, it was allowed to melt overnight by raising the temperature above the freezing point. Some ice still had to be recovered the next day, before the diesel tests were started. Diesel was again pumped in to achieve a 30 mm thick layer. Although the diesel mixed with some of the residual Endicott in the tank and tank walls, the viscosity of the diesel was still quite low at these freezing conditions, around 4 to 6 cP.

Given its much lower viscosity, the discrepancies between the grooves and the cleaning blades became much more apparent and significant. After a few runs with the $20^o$ and $40^o$ drums, it became apparent that too much diesel was being lost by the mismatch between the blade and the drum. This probably also influenced the results with Endicott and HydroCal, but to a much lesser extent due to their higher viscosity. The results of these tests with the $20^o$ and $40^o$ drums are not presented, since they would provide an inaccurate representation of their performance. Even for the other Mini Max drums (Aluminum $30^o$, Neoprene $30^o$ and flat drum), pressure had to be applied on the cleaning blade to ensure a good fit with the drum. It is recommended that the cleaning blades be perfectly matched to the grooved drums, and that the spring pressure be incremented to maintain a tight fit. Due to time limitations, only a few runs were performed with diesel. However, the performance of the Mini Max and the PE 118 were established with these runs (Figure 48).

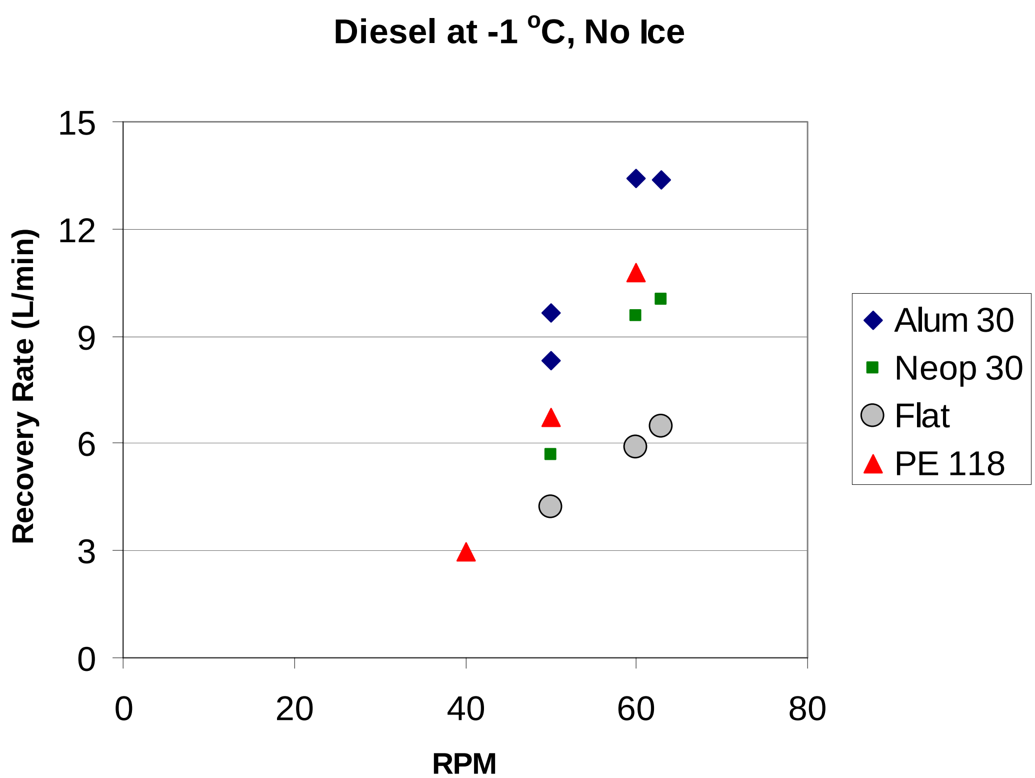


**Figure 48. Recovery rates for diesel at -1 °C, in the absence of ice. Recovery rate after subtracting any free or emulsified water. Data for one drum recovering oil.**

Overall, the recovery of the Aluminum $30^o$ grooved drum was the highest, probably due to the better match between the cleaning blade and the drum. The maximum recovery rate was reached at around 60 rpm, since increasing the speed to 63 rpm did not increase the recovery rate of diesel. The duplicate test at 50 rpm for the Aluminum $30^o$ drum indicated some variability (± 0.7 L/min) from run to run, probably due to the manual pressure application on the cleaning blade. The performance of the PE 118 drum was linear within the range tested (40 to 60 rpm), and although somewhat lower than for the Aluminum 30$^o$ drum, it was still well above the flat drum at the higher rpm. There was essentially no emulsification of diesel, and the amount of water recovered in these tests without ice was minimal, less than 1%.

In the last few hours available during the last test day, ice was added to diesel to achieve a 30% by weight mixture. Although the ice tends to disappear below the diesel layer, periodic sampling of the mixture in the tank indicated that the ice was relative homogeneously distributed, with few large ice clusters. As observed before, recovery of the diesel/ice mixture did not result in significant ice buildup around the recovery point. In general, much less ice was lifted out of the surface, given the low viscosity of diesel. The few tests performed under these conditions ranged from 0 to 5% free water, indicating some ice was recovered in some of the tests but none in others. The water content of the diesel oil was between 0.01 and 0.04%, indicating very little or no emulsification. The PE 118 skimmer had to be packed for shipment before these tests, so it was not possible to test it with diesel and ice. The results (Figure 49) indicate that the grooved Aluminum 30$^o$ drum performed quite well even in the presence of ice, considerably better than the flat drum. In fact the recovery rates for this drum were around the same with or without ice. Figures 50 and 51 present the recovery of diesel with grooved and flat drums. The diesel had a medium brown hue due to the film of Endicott left in the test tank. Note that the grooves are only filled to at most 30-40% of their capacity with the 30$^o$ drum.

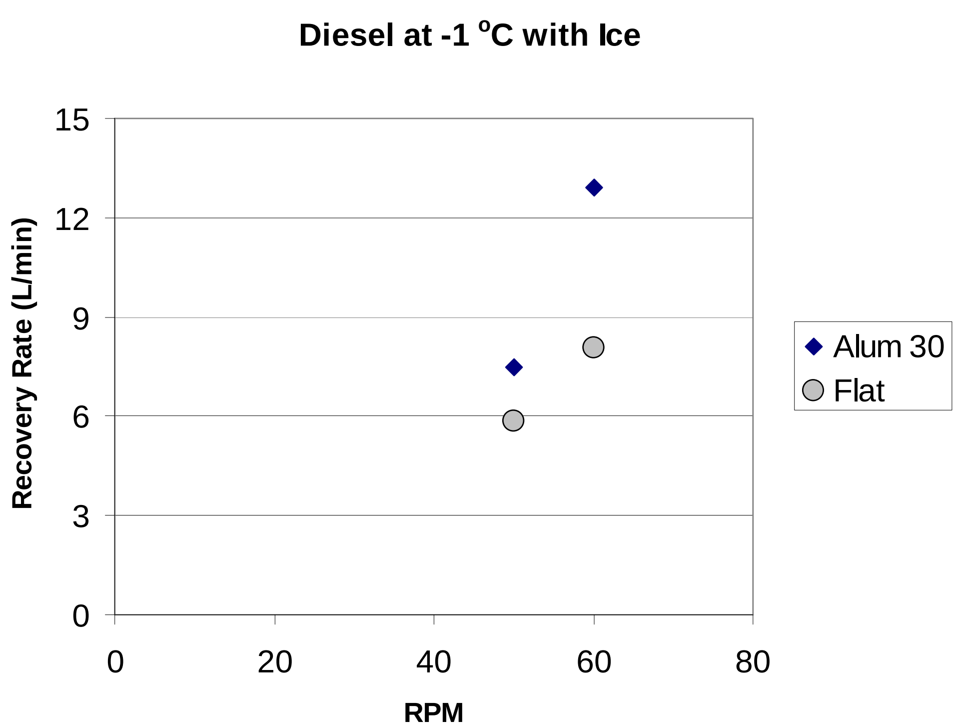


**Figure 49. Recovery rates for diesel at -1 $^o$C with ice present at 30% by weight. Recovery rate after subtracting any free or emulsified water. Data for one drum recovering oil.**

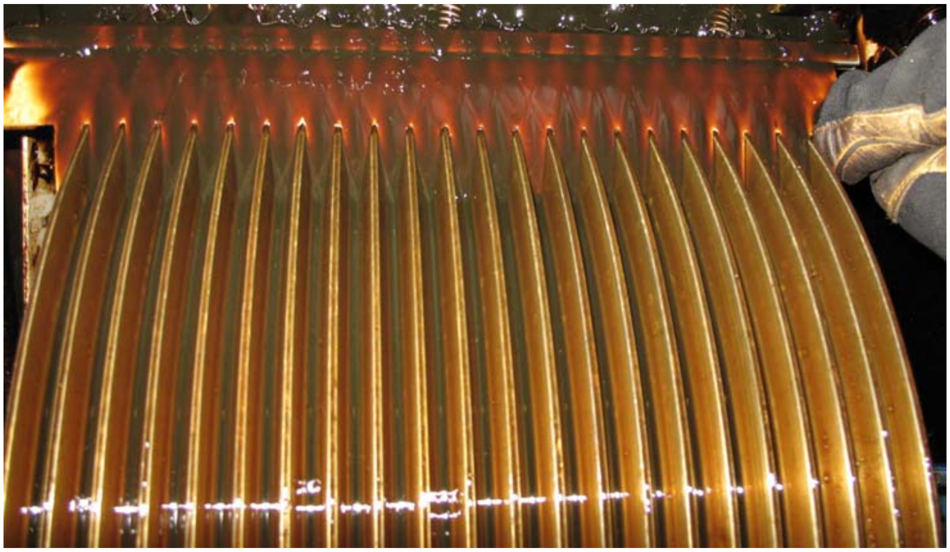

**Figure 50. Recovery of diesel with the 30$^o$ grooved drum. Note that only a fraction of the groove is occupied with diesel, indicating that a narrower groove would recover significantly more diesel.**

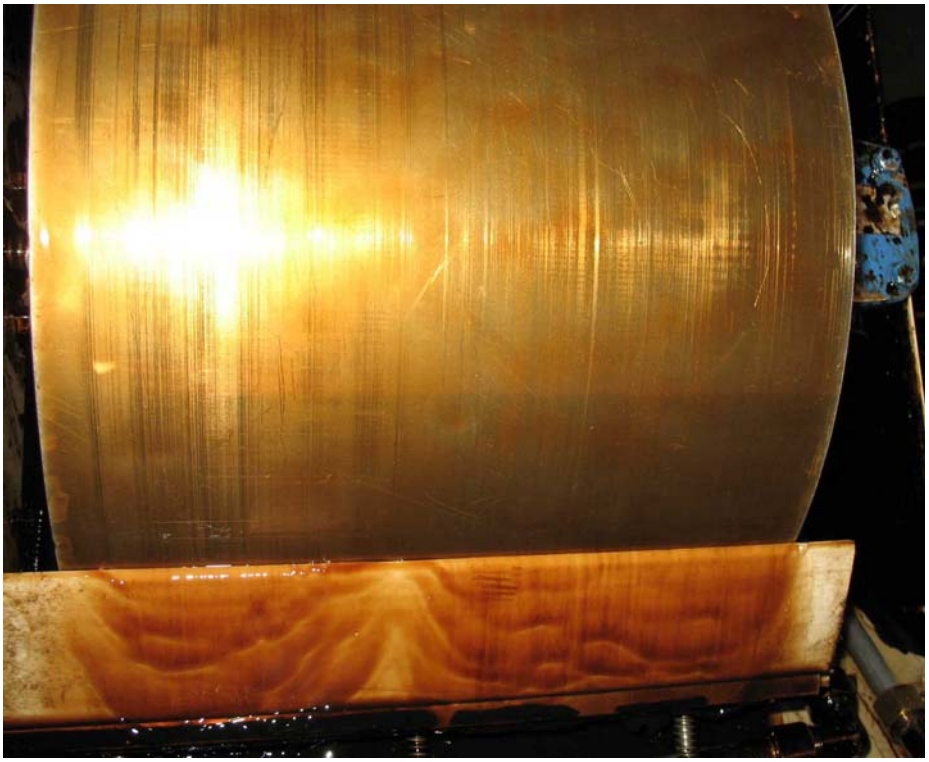

**Figure 51. Recovery of diesel with the flat drum. Only a thin film of diesel coats the drum.**

## 5. Conclusions and Recommendations

The objectives of this research were to understand the behavior of oils and oil/ice mixtures in cold climate conditions in order to improve oil spill recovery, and to determine whether the recent significant improvements in skimmer design would work adequately under these cold climate conditions. Both of these objectives were fully met.

The laboratory experiments provide important insights into the key physicochemical properties that control the behavior of oil and oil/ice mixtures under these conditions. Although it is well known that viscosity is a strong function of temperature, it was clear that under these conditions, every degree that the temperature decreases can have a significant effect on viscosity, since the relationship is semi-logarithmic for all oils tested. The incorporation of ice into the mixture can have different effects, depending on whether the initial oil viscosity is low, such as with diesel and fresh Endicott, or high as is the case for HydroCal 300 and weathered Endicott. For low viscosity oils, the oil/ice mixture is not cohesive, and thus the effect on viscosity is important, but not as significant as is the case for higher viscosity oils. In the case of HydroCal 300, the formation of a cohesive mixture increases significantly the viscosity, while in the case of the very viscous weathered Endicott the presence of ice actually seems to provide lubrication, reducing the viscosity up to a certain point. It was also interesting to observe how a colder fresh Endicott (-5 oC) would behave more similarly to higher viscosity oils, with the formation of a more cohesive oil/ice mixture and a sharp increase in viscosity with increasing ice content. The effect of temperature or ice content on density or surface tension was much less significant, and is almost negligible for oil/ice mixtures that are not cohesive.

The evaluation of different materials served to determine which surfaces would perform better under different conditions, and extended our previous work at higher temperatures (Broje and Keller, 2007b). Under cold climate conditions in the laboratory, Neoprene and other elastomers (Hypalon and SBR) had higher oil mass recovery from an oil film, compared to hard polymers (LDPE) and metals (aluminum). Thus, Neoprene and Hypalon coated drums were considered in the CRREL field tests. Although a lower contact angle in indicative of better wetting, the correlation between contact angle and oil recovery was not very clear. It is recommended that mass recovery be used as the parameter that can best determine whether a material will be better than others for oil recovery.

The field tests at CRREL were very successful. All the drums performed well under oil only and oil/ice conditions. In general, there was only a small difference in recovery between drums of different materials, although this may also reflect small but important differences in the fit between the cleaning blade and the grooved drums, since a less than optimal fit resulted in some loss of recovered material. This was particularly noticeable for the lighter oils (Endicott and diesel), and for the $20^o$ and $40^o$ grooved drums. All the grooved drums performed substantially better than the traditional flat drums used in common practice.

Although the recovery of oil/ice mixtures was quite satisfactory, the presence of ice did reduce to a noticeable extent the recovery of oil, not just because the drums were recovering oil and ice which eventually would melt to water, but due to the fact that part of the groove was filled with ice particles. The decrease in oil recovery rate is more significant at higher ice content, and for more viscous oils. One important finding is that ice did not seem to accumulate behind the skimmer during the tests, although this may also be related to the thickness of the oil layer (25 ± 5 mm).

Given the relatively low cost of retrofitting existing skimmers with the new grooved drums, it is recommendable that a program to replace them be promoted, since this can improve the rate of oil recovery and reduce the risk of a spill reaching valuable resources.

## 6. Acknowledgements

The authors would like to thank the two funding agencies, the Coastal Response Research Center, Cooperative Institute for Coastal and Estuarine Environmental Technology, Prince William Sound Oil Spill Recovery Institute, and the Department of the Interior, Minerals Management Service, for their support. We would also like to thank Joseph Mullin from the Minerals Management Service, for his insights, support and assistance in obtaining the crude oils used in these tests; Leonard Zabilansky from CRREL for his advice and support during the tests, as well as obtaining permission from CRREL to do the work at the MEF; Marie Darling from CRREL to the list for assisting in the logistics and public relations for the CRREL tests; Donnie Wilson and Jeff Cantrell from American Elastec/American Marine, for donating valuable time during the field tests, as well as providing the PE-118 skimmer for the testing; Bill Schmidt, Alan Guarino and Don Snyder from Mar, Inc., for their help and support during the CRREL tests; Victoria Broje, now at Shell Global Solutions for her insights; Lee Majors and Ken Linderman from Alaska Clean Seas for their help with obtaining Endicott oil; and Will Lewis and Jennifer Paludi for all the hard work in the laboratory under cold climate conditions.

Dr. Keller would in particular like to thank Kristin Clark, for conducting many of the cold climate experiments and her professionalism during the CRREL tests.

## 7. Literature Cited

Broje V. and A. A. Keller, 2006. Improved Mechanical Oil Spill Recovery Using an Optimized Geometry for the Skimmer Surface. Environ. Sci. Tech. 40(23):7914-7918

Broje V. and A. A. Keller, 2007a. Effect of Operational Parameters on the Recovery Rate of an Oleophilic Drum Skimmer. J. Haz. Matls, doi:10.1016/j.jhazmat.2007.02.017.

Broje V. and A. A. Keller, 2007b. Interfacial interactions between hydrocarbon liquids and solid surfaces used in mechanical oil spill recovery. J. Colloid & Interface Science, 305:286–292, doi:10.1016/j.jcis.2006.09.078

Della Bona A., Shen C. and Anusavice K.J., 2004. Work of adhesion of resin on treated lithia disilicate-based ceramic, Dental Materials, 20:4

Lee Y., Fang T., Yang Y. and Maa J., 1998. The enhancement of dropwise condensation by wettability modification of solid surface, International Communications in Heat and Mass Transfer, 25:8.

Wake W.C., 1982. Adhesion and the formulation of adhesives. Applied Science Publishers, London.

## Appendix A. Complete Field Tests Results

| Test<br>#  | Test Description<br>Drum – oil – ice | Slick Thick<br>mm | Rot. Speed<br>RPM | Air T<br>°C | Wat T<br>°C | Oil Visc.<br>cP | Recov. Time<br>sec | Total Fluids Recov<br>L | Total Recov. Rate<br>L/min | Free Water<br>vol % | Emulsif Water<br>vol. % | Decant Water<br>vol % | Oil Recov. Rate<br>L/min |
|---|---|---|---|---|---|---|---|---|---|---|---|---|---|
| 1 | Alum 20° – HydroCal – no ice | 25 | 20 | -1.7 | -1.1 | 909 | 120 | 81 | 40.3 | 0.0% | 0.02% | 0% | 40.3 |
| 2 | Alum 20° – HydroCal – no ice | 25 | 15 | -1.5 | -1.1 | 1006 | 120 | 62 | 30.8 | 0.0% | 0.02% | 0% | 30.8 |
| 3 | Alum 20° – HydroCal – no ice | 25 | 10 | -1.5 | -1.1 | 1289 | 120 | 40 | 19.9 | 0.0% | 0.01% | 0% | 19.9 |
| 4 | Alum 30° – HydroCal – no ice | 25 | 20 | -0.6 | -1.1 | 1230 | 120 | 106 | 53.2 | 0.0% | 0.01% | 0% | 53.2 |
| 5 | Alum 30° – HydroCal – no ice | 25 | 15 | -2.6 | -1.1 | 1124 | 120 | 71 | 35.6 | 0.0% | 0.02% | 0% | 35.6 |
| 6 | Alum 30° – HydroCal – no ice | 25 | 10 | -2.6 | -1.1 | 1222 | 120 | 44 | 21.8 | 0.0% | 0.02% | 0% | 21.8 |
| 7 | Alum 30° – HydroCal – no ice | 25 | 20 | -2.6 | -1.1 | 1212 | 120 | 106 | 53.2 | 0.0% | 0.01% | 0% | 53.2 |
| 8 | Alum 40° – HydroCal – no ice | 25 | 10 | -2.1 | -1.1 | 1257 | 120 | 40 | 20.2 | 0.0% | 0.01% | 0% | 20.2 |
| 9 | Alum 40° – HydroCal – no ice | 25 | 15 | -2.2 | -1.1 | 1286 | 120 | 70 | 35.0 | 0.0% | 0.01% | 0% | 35.0 |
| 10 | Alum 40° – HydroCal – no ice | 25 | 20 | -2.2 | -1.1 | 1116 | 120 | 97 | 48.4 | 0.0% | 0.01% | 0% | 48.4 |
| 11 | Neop 30° – HydroCal – no ice | 25 | 30 | -1.6 | -1.1 |  | 120 | 98 | 49.2 | 0.3% | 0.03% | 0% | 49.0 |
| 12 | Neop 30° – HydroCal – no ice | 25 | 30 | -2.0 | -1.1 | 1185 | 120 | 106 | 53.0 | 0.6% | 0.05% | 0% | 52.7 |
| 13 | Neop 30° – HydroCal – no ice | 25 | 20 | -2.0 | -1.1 | 1173 | 120 | 98 | 49.2 | 0.8% | 0.06% | 0% | 48.8 |
| 14 | Neop 30° – HydroCal – no ice | 25 | 10 | -1.7 | -1.1 | 1118 | 120 | 48 | 24.2 | 0.6% | 0.07% | 0% | 24.1 |
| 15 | Neop 30° – HydroCal – no ice | 25 | 15 | -1.6 | -1.1 | 942 | 120 | 75 | 37.5 | 1.5% | 0.03% | 0% | 36.9 |
| 16 | Hypa 30° – HydroCal – no ice | 25 | 10 | -1.6 | -1.1 | 1032 | 120 | 40 | 20.1 | 0.0% | 0.02% | 0% | 20.1 |
| 17 | Hypa 30° – HydroCal – no ice | 25 | 15 | -1.6 | -1.1 | 1222 | 120 | 66 | 33.1 | 0.0% | 0.03% | 0% | 33.1 |
| 18 | Hypa 30° – HydroCal – no ice | 25 | 20 | -1.6 | -1.1 | 1095 | 120 | 98 | 49.0 | 0.0% | 0.02% | 0% | 49.0 |
| 19 | Flat – HydroCal – no ice | 25 | 20 | -1.0 | -1.1 | 1127 | 120 | 44 | 21.8 | 0.0% | 0.02% | 0% | 21.8 |
| 20 | Flat – HydroCal – no ice | 25 | 10 | -1.4 | -1.1 | 1011 | 120 | 30 | 15.2 | 0.0% | 0.02% | 0% | 15.2 |
| 21 | Alum 20° – HydroCal – w/ice | 25 | 10 | -1.5 | -1.1 | 1304 | 120 | 34 | 17.0 | 2.1% | 0.06% | 0% | 16.6 |
| 22 | Alum 20° – HydroCal – w/ice | 25 | 15 | -1.5 | -1.1 | 1351 | 120 | 46 | 23.0 | 3.0% | 0.02% | 0% | 22.3 |
| 23 | Alum 20° – HydroCal – w/ice | 25 | 20 | -1.5 | -1.1 | 1305 | 120 | 45 | 22.3 | 6.6% | 0.02% | 0% | 20.8 |
| 24 | Alum 20° – HydroCal – w/ice | 25 | 15 | -2.1 | -2.2 | 1113 | 120 | 41 | 20.5 | 5.3% | 0.01% | 0% | 19.4 |
| 25 | Alum 30° – HydroCal – w/ice | 25 | 10 | -2.1 | -2.2 | 1243 | 120 | 40 | 19.8 | 3.8% | 0.01% | 0% | 19.1 |
| 26 | Alum 30° – HydroCal – w/ice | 25 | 15 | -2.1 | -2.2 | 1289 | 120 | 58 | 29.0 | 3.6% | 0.01% | 0% | 28.0 |
| 27 | Alum 30° – HydroCal – w/ice | 25 | 20 | -2.1 | -2.2 | 1236 | 120 | 70 | 34.9 | 4.4% | 0.01% | 0% | 33.4 |
| 28 | Alum 40° – HydroCal – w/ice | 25 | 12 | -1.4 | -1.1 | 1451 | 120 | 25 | 12.6 | 7.3% | 0.01% | 0% | 11.6 |
| 29 | Alum 40° – HydroCal – w/ice | 25 | 14 | -1.4 | -1.1 | 1217 | 120 | 37 | 18.5 | 10.0% | 0.01% | 0% | 16.6 |
| 30 | Alum 40° – HydroCal – w/ice | 25 | 16 | -1.4 | -1.1 | 1701 | 120 | 42 | 21.1 | 5.1% | 0.01% | 0% | 20.0 |
| 31 | Alum 40° – HydroCal – w/ice | 25 | 15 | -2.0 | -2.2 | 918 | 120 | 40 | 19.8 | 9.2% | 0.01% | 0% | 18.0 |
| 32 | Flat – HydroCal – w/ice | 25 | 15 | -2.0 | -2.2 | 1413 | 120 | 33 | 16.6 | 7.8% | 0.01% | 0% | 15.3 |
| 33 | Flat – HydroCal – w/ice | 25 | 10 | -2.0 | -2.2 | 987 | 120 | 20 | 9.8 | 2.6% | 0.01% | 0% | 9.6 |
| 34 | 118 PE – HydroCal – w/ice | 25 | 20 | -2.0 | -2.2 | 1290 | 120 | 89 | 44.7 | 10.7% | 0.01% | 0% | 40.0 |
| 35 | 118 PE – HydroCal – w/ice | 25 | 15 | -2.0 | -2.2 | 1515 | 120 | 72 | 35.9 | 12.8% | 0.01% | 0% | 31.3 |

| Test | Test Description | Slick Thick | Rot. Speed | Air T | Wat T | Oil Visc. | Recov. Time | Total Fluids Recov | Total Recov. Rate | Free Water | Emulsif Water | Decant Water | Oil Recov. Rate |
|---|---|---|---|---|---|---|---|---|---|---|---|---|---|
| # | Drum – oil – ice | mm | RPM | $^{o}$C | $^{o}$C | cP | sec | L | L/min | vol % | vol. % | vol % | L/min |
| 36 | 118 PE – HydroCal – w/ice | 25 | 10 | -2.0 | -2.2 | 1341 | 120 | 48 | 24.2 | 5.6% | 0.01% | 0% | 22.9 |
| 37 | Alum 20$^{o}$ – Endicott – no ice | 25 | 30 | 0.1 | -1.7 | 279 | 120 | 77 | 38.7 | 2.5% | 0.47% | 0% | 37.6 |
| 38 | Alum 20$^{o}$ – Endicott – no ice | 25 | 40 | 0.2 | -1.7 | 282 | 120 | 125 | 62.5 | 1.3% | 0.23% | 0% | 61.6 |
| 39 | Alum 20$^{o}$ – Endicott – no ice | 25 | 50 | 0.2 | -1.7 | 296 | 60 | 78 | 77.6 | 3.9% | 1.04% | 0% | 73.7 |
| 40 | Alum 30$^{o}$ – Endicott – no ice | 25 | 20 | 0.2 | -1.7 | 264 | 60 | 27 | 26.9 | 1.5% | 0.38% | 0% | 26.4 |
| 41 | Alum 30$^{o}$ – Endicott – no ice | 25 | 30 | 0.2 | -1.7 | 265 | 60 | 44 | 44.4 | 2.3% | 0.54% | 0% | 43.1 |
| 42 | Alum 30$^{o}$ – Endicott – no ice | 25 | 40 | 0.2 | -1.7 | 315 | 60 | 55 | 55.0 | 1.4% | 0.96% | 0% | 53.7 |
| 43 | Alum 30$^{o}$ – Endicott – no ice | 25 | 40 | -0.5 | -1.7 |  | 90 | 93 | 61.9 | 1.4% | 3.45% | 0% | 59.0 |
| 44 | Alum 30$^{o}$ – Endicott – no ice | 25 | 50 | -0.5 | -1.7 | 324 | 90 | 123 | 81.7 | 1.5% | 1.72% | 0% | 79.1 |
| 45 | Alum 30$^{o}$ – Endicott – no ice | 25 | 30 | 0.2 | -1.7 | 431 | 120 | 98 | 49.2 | 1.6% | 1.14% | 0% | 47.8 |
| 46 | Alum 40$^{o}$ – Endicott – no ice | 25 | 50 | 0.2 | -1.7 | 302 | 60 | 82 | 82.2 | 3.0% | 0.75% | 0% | 79.1 |
| 47 | Alum 40$^{o}$ – Endicott – no ice | 25 | 40 | 0.2 | -1.7 | 315 | 90 | 93 | 61.9 | 3.8% | 0.80% | 0% | 59.1 |
| 48 | Alum 40$^{o}$ – Endicott – no ice | 25 | 30 | 0.2 | -1.7 | 275 | 120 | 70 | 35.2 | 2.6% | 0.88% | 0% | 34.0 |
| 49 | Neop 30$^{o}$ – Endicott – no ice | 25 | 40 | 0.2 | -1.7 | 310 | 73 | 75 | 61.7 | 2.6% | 0.21% | 0% | 60.0 |
| 50 | Neop 30$^{o}$ – Endicott – no ice | 25 | 30 | 0.2 | -1.7 | 361 | 120 | 96 | 48.1 | 2.2% | 0.26% | 0% | 46.9 |
| 51 | Neop 30$^{o}$ – Endicott – no ice | 25 | 50 | 0.2 | -1.7 | 449 | 62 | 84 | 81.1 | 2.9% | 0.89% | 0% | 78.1 |
| 52 | Hypa 30$^{o}$ – Endicott – no ice | 25 | 30 | 0.2 | -1.7 | 329 | 120 | 40 | 19.9 | 1.4% | 0.49% | 0% | 19.5 |
| 53 | Flat – Endicott – no ice | 25 | 30 | 0.2 | -1.7 | 324 | 120 | 37 | 18.5 | 2.9% | 0.31% | 0% | 17.9 |
| 54 | Flat – Endicott – no ice | 25 | 40 | 0.2 | -1.7 | 318 | 120 | 55 | 27.4 | 3.6% | 0.25% | 0% | 26.4 |
| 55 | 118 PE – Endicott – no ice | 25 | 30 | 0.2 | -1.7 | 280 | 120 | 116 | 58.1 | 3.6% | 1.36% | 0% | 55.2 |
| 56 | 118 PE – Endicott – no ice | 25 | 40 | 0.2 | -1.7 | 243 | 60 | 88 | 87.8 | 2.7% | 1.77% | 0% | 83.9 |
| 57 | 118 PE – Endicott – no ice | 25 | 50 | 0.2 | -1.7 | 366 | 60 | 123 | 122.6 | 1.4% | 0.98% | 0% | 119.7 |
| 58 | 118 PE – Endicott – no ice | 25 | 63 | 0.2 | -1.7 | 332 | 60 | 145 | 144.8 | 2.1% | 0.66% | 0% | 140.8 |
| 59 | Alum 20$^{o}$ – Endicott – w/ice | 25 | 20 | -2.9 | -2.2 | 655 | 60 | 34 | 34.0 | 7.7% | 15.18% | 0% | 26.2 |
| 60 | Alum 20$^{o}$ – Endicott – w/ice | 25 | 30 | -2.9 | -2.2 | 502 | 60 | 55 | 55.1 | 7.9% | 9.01% | 0% | 45.7 |
| 61 | Alum 20$^{o}$ – Endicott – w/ice | 25 | 40 | -2.9 | -2.2 | 563 | 60 | 69 | 69.5 | 11.2% | 9.71% | 0% | 54.9 |
| 62 | Alum 30$^{o}$ – Endicott – w/ice | 25 | 40 | -2.9 | -2.2 | 610 | 60 | 76 | 75.8 | 4.2% | 8.40% | 0% | 66.3 |
| 63 | Alum 30$^{o}$ – Endicott – w/ice | 25 | 30 | -2.9 | -2.2 | 500 | 120 | 108 | 53.8 | 7.8% | 8.84% | 0% | 44.9 |
| 64 | Alum 30$^{o}$ – Endicott – w/ice | 25 | 20 | -2.9 | -2.2 | 545 | 120 | 71 | 35.5 | 9.2% | 9.30% | 0% | 29.0 |
| 65 | Alum 40$^{o}$ – Endicott – w/ice | 25 | 30 | -1.2 | -1.1 | 604 | 120 | 93 | 46.7 | 21.4% | 8.84% | 0% | 32.6 |
| 66 | Alum 40$^{o}$ – Endicott – w/ice | 25 | 40 | -1.2 | -1.1 | 512 | 60 | 74 | 74.3 | 4.9% | 9.79% | 0% | 63.4 |
| 67 | Alum 40$^{o}$ – Endicott – w/ice | 25 | 50 | -1.2 | -1.1 | 534 | 60 | 74 | 74.3 | 16.9% | 13.70% | 0% | 51.6 |
| 68 | Alum 40$^{o}$ – Endicott – w/ice | 25 | 20 | -3.5 | -2.2 | 584 | 60 | 36 | 35.6 | 9.5% | 8.51% | 0% | 29.2 |
| 69 | Alum 40$^{o}$ – Endicott – w/ice | 25 | 30 | -3.5 | -2.2 | 660 | 60 | 60 | 60.0 | 7.1% | 12.04% | 0% | 48.5 |
| 70 | Alum 40$^{o}$ – Endicott – w/ice | 25 | 40 | -3.5 | -2.2 | 741 | 60 | 64 | 63.8 | 10.3% | 4.70% | 0% | 54.3 |
| 71 | Flat – Endicott – w/ice | 25 | 20 | -2.8 | -2.2 | 568 | 60 | 12 | 12.2 | 9.1% | 11.74% | 0% | 9.7 |
| 72 | Flat – Endicott – w/ice | 25 | 40 | -2.8 | -2.2 | 638 | 60 | 42 | 41.9 | 8.5% | 6.58% | 0% | 35.6 |
| 73 | Flat – Endicott – w/ice | 25 | 30 | -2.8 | -2.2 | 719 | 60 | 24 | 24.4 | 9.4% | 10.23% | 0% | 19.6 |
| 74 | 118 PE – Endicott – w/ice | 25 | 40 | -2.8 | -2.2 | 635 | 60 | 81 | 81.3 | 8.8% | 7.73% | 0% | 67.8 |
| 75 | 118 PE – Endicott – w/ice | 25 | 30 | -2.8 | -2.2 | 491 | 60 | 81 | 80.6 | 8.8% | 10.74% | 0% | 64.9 |

| Test<br>#| Test Description<br>Drum – oil – ice | Slick Thick<br>mm | Rot. Speed<br>RPM | Air T<br>°C | Wat T<br>°C | Oil Visc.<br>cP | Recov. Time<br>sec | Total Fluids Recov<br>L | Total Recov. Rate<br>L/min | Free Water<br>vol % | Emulsif Water<br>vol. % | Decant Water<br>vol % | Oil Recov. Rate<br>L/min |
|---|---|---|---|---|---|---|---|---|---|---|---|---|---|
| 76 | 118 PE – Endicott – w/ice | 25 | 20 | -2.8 | -2.2 | 615 | 60 | 48 | 47.6 | 4.0% | 13.16% | 0% | 39.5 |
| 77 | Alum 20° – Diesel – no ice | 25 | 30 | -0.2 | -1.1 | 5.51 | 180 | 1 | 0.4 | 0.0% | 0.01% | 0% | 0.4 |
| 78 | Alum 30° – Diesel – no ice | 25 | 50 | -3.4 | -1.1 | 5.46 | 180 | 25 | 8.4 | 0.7% | 0.01% | 0% | 8.3 |
| 79 | Alum 30° – Diesel – no ice | 25 | 50 | -3.4 | -1.1 | 5.31 | 240 | 39 | 9.6 | 0.0% | 0.01% | 0% | 9.6 |
| 80 | Alum 30° – Diesel – no ice dup | 25 | 60 | -3.1 | -1.1 | 5.34 | 180 | 40 | 13.5 | 0.6% | 0.01% | 0% | 13.4 |
| 81 | Alum 30° – Diesel – no ice | 25 | 63 | -3.1 | -1.1 | 6.00 | 180 | 40 | 13.5 | 0.7% | 0.01% | 0% | 13.4 |
| 82 | Neop 30° – Diesel – no ice | 25 | 50 | -1.8 | -1.1 | 4.77 | 240 | 23 | 5.7 | 0.0% | 0.01% | 0% | 5.7 |
| 83 | Neop 30° – Diesel – no ice | 25 | 60 | -1.8 | -1.1 | 4.71 | 180 | 29 | 9.6 | 0.0% | 0.01% | 0% | 9.6 |
| 84 | Neop 30° – Diesel – no ice | 25 | 63 | -1.8 | -1.1 | 4.52 | 180 | 30 | 10.0 | 0.0% | 0.01% | 0% | 10.0 |
| 85 | Flat – Diesel – no ice | 25 | 50 | -2.6 | -1.1 | 4.71 | 300 | 21 | 4.2 | 0.0% | 0.01% | 0% | 4.2 |
| 86 | Flat – Diesel – no ice | 25 | 60 | -2.6 | -1.1 | 4.71 | 300 | 30 | 5.9 | 0.0% | 0.01% | 0% | 5.9 |
| 87 | Flat – Diesel – no ice | 25 | 63 | -2.6 | -1.1 | 4.74 | 300 | 32 | 6.5 | 0.0% | 0.01% | 0% | 6.5 |
| 88 | 118 PE – Diesel – no ice | 25 | 60 | -2.6 | -1.1 | 3.84 | 180 | 32 | 10.8 | 0.0% | 0.01% | 0% | 10.8 |
| 89 | 118 PE – Diesel – no ice | 25 | 50 | -2.6 | -1.1 | 4.14 | 240 | 27 | 6.8 | 0.5% | 0.01% | 0% | 6.7 |
| 90 | 118 PE – Diesel – no ice | 25 | 40 | -2.6 | -1.1 | 4.68 | 300 | 15 | 3.0 | 0.0% | 0.01% | 0% | 3.0 |
| 91 | Alum 30° – Diesel – w/ice | 25 | 50 | -2.6 | -1.7 | 4.29 | 180 | 24 | 7.9 | 5.2% | 0.04% | 0% | 7.5 |
| 92 | Alum 30° – Diesel – w/ice | 25 | 60 | -2.6 | -1.7 | 4.29 | 180 | 39 | 12.9 | 0.0% | 0.01% | 0% | 12.9 |
| 93 | Flat – Diesel – w/ice | 25 | 60 | -2.6 | -1.7 | 4.38 | 300 | 40 | 8.0 | 0.0% | 0.01% | 0% | 8.0 |
| 94 | Flat – Diesel – w/ice | 25 | 50 | -2.6 | -1.7 | 4.29 | 300 | 29 | 5.8 | 0.0% | 0.01% | 0% | 5.8 |

**Appendix B. Karl Fischer Titration and Free Water Content Procedures**

Start of the Day

1. Empty titration vessel
2. Clean with diesel (magnetic stir bar, tubing, titration vessel)
3. Re-assemble
4. Rinse the tip of the burette
5. Dispense 2 mLs of titrant into waste bottle
6. Pump fresh solvent into titration vessel (variable amounts min= 40mL)
7. Run Method 8 (arbitrary program number)

Method 8

1. Run drift (5 minutes)
2. Check concentration of titrant using water standard 5 (5mL = 5 mg $H_2O$)
    a. Use Finnpipette to add 2 to 3 mL of water standard 5
    b. Reaction in titration vessel takes less than a minute
    c. Store the [titrant] if within acceptable range
3. Run sample
    a. initial guess 0.5% water content
    b. add sample in range of 0-5 grams
        i. add as close to 5 grams as possible using luer lock 5 mL syringe
        ii. weigh before and after addition of sample for mass balance
    c. proceed with automated titration
        i. % water content result appears
        ii. or message "Endpoint not reached termination through $V_{max}$"
            1. termination controls set at 20 mL of titrant or 10 minutes
            2. if reaction exceeds either one of those conditions the reaction is terminated
            3. due to excess water content in titration vessel and reaction will take too long for accurate drift
            4. correct by pumping out titration vessel and guessing higher water content value and adding ~1 gram of sample
            5. continue until guess meets range of sample
4. Recalculate % water content
    a. Using true mass of sample added recalculate % water content
    b. Record this value
5. Every 10 samples perform the titration with water standard 5 to correct for variable water influx in titrant and solvent
6. Leave on standby mode between runs to continually titrate water in titration vessel (uses very minimal amount of titrant)

Mettler-Toledo KF instrument automatically calculates the range of sample to add based on the titrant concentration and the burette volume of 5mL, in all cases except the low concentrations like 0.05% or less the upper bound limit of sample was added. For the low percent water content values a significant amount of 14-18 grams of sample was added but not the 36 to 70 grams of the upper bound.

Measuring Free Water Content

1. After the sample has been added to the titration vessel in 5 mL or 500µL syringe aliquots decant off the top layer of oil into the 200 mL Nalgene graduated cylinder meeting accuracy requirements of ASTM class B cylinders.
    a. Record the volume of oil in grad cylinder
2. The layer of oil and free water is then slowly poured into a 50 mL graduated cylinder.
    a. Record oil and water volume in 50 mL grad cylinder
3. Pipet out the free water into another grad cylinder
4. Subtract the free water volume from the initial volume recording
5. Add in the volume of oil used for rinsing the syringe 3 times prior to sample injection and the amount used for the sample.
6. Total the water and oil values and record.

## Appendix C. Actual groove dimensions

| Drum | # Grooves | Drum Width (mm) | Groove Width (mm) | Depth (mm) | Actual Angle (degrees) |
|---|---|---|---|---|---|
| 20 Aluminum | 28 | 215.9 | 7.30 | 12.96 | 31.5 |
| 30 Aluminum | 21 | 215.9 | 10.50 | 15.00 | 38.6 |
| 30 Neoprene | 21 | 215.9 | 10.50 | 15.00 | 38.6 |
| 30 Hypalon | 21 | 215.9 | 10.50 | 15.00 | 38.6 |
| 40 Aluminum | 16 | 215.9 | 13.52 | 14.88 | 48.9 |
| 118 Polyethylene | 21 | 423.08 | 19.84 | 12.70 | 76.0 |